



# AMERICAN METEOROLOGICAL SOCIETY

*Journal of Hydrometeorology*

## **EARLY ONLINE RELEASE**

This is a preliminary PDF of the author-produced manuscript that has been peer-reviewed and accepted for publication. Since it is being posted so soon after acceptance, it has not yet been copyedited, formatted, or processed by AMS Publications. This preliminary version of the manuscript may be downloaded, distributed, and cited, but please be aware that there will be visual differences and possibly some content differences between this version and the final published version.

The DOI for this manuscript is doi: 10.1175/JHM-D-12-083.1

The final published version of this manuscript will replace the preliminary version at the above DOI once it is available.

If you would like to cite this EOR in a separate work, please use the following full citation:

Rebora, N., L. Molini, E. Casella, A. Comellas, E. Fiori, F. Pignone, F. Siccardi, F. Silvestro, S. Tanelli, and A. Parodi, 2013: Extreme rainfall in the Mediterranean: what can we learn from observations?. *J. Hydrometeor.* doi:10.1175/JHM-D-12-083.1, in press.



# 1 Extreme rainfall in the Mediterranean: what can 2 we learn from observations?

3  
4 Rebora, N.<sup>(1)</sup>, Molini, L.<sup>(1)</sup>, Casella, E.<sup>(1),(3)</sup>, Comellas, A.<sup>(1),(3)</sup>,  
5 Fiori, E.<sup>(1),(3)</sup>, Pignone, F.<sup>(1),(3)</sup>, Siccardi, F.<sup>(1),(3)</sup>, Silvestro, F.<sup>(1)</sup>,  
6 Tanelli, S.<sup>(2)</sup>, and Parodi, A.<sup>(1)</sup>

7  
8 (1) CIMA Research Foundation, Savona, Italy

9 (2) Jet Propulsion Laboratory, California Institute of Technology,  
10 Pasadena, California, US

11 (3) University of Genoa, Italy

12  
13  
14  
15  
16  
17  
18  
19  
20  
21  
22  
23  
24  
25  
26  
27  
28  
29  
30  
31  
32  
33  
34  
35 

---

*Corresponding author address: Nicola Rebora*, CIMA Research Foundation, via Magliotto 2, 17100.,  
36 Savona, Italy.

37 E-mail: [nicola.rebora@cimafoundation.org](mailto:nicola.rebora@cimafoundation.org)  
38

1 Abstract

2  
3 Flash-floods induced by extreme rainfall events represent one of the most life-  
4 threatening phenomena in the Mediterranean. While their catastrophic ground effects are  
5 well documented by post-event surveys, the extreme rainfall events that generate them  
6 are still difficult to observe properly.

7 Being able to collect observations on such events will help scientists in better  
8 understand and model these phenomena. The recent flash-floods that hit Liguria Region  
9 (Italy) between the end of October and the beginning of November 2011 give us the  
10 opportunity to use the measurements available from a large number of sensors, both  
11 ground based and spaceborne, to characterize these events.

12 In this paper we analyze the role of the key ingredients (e.g. unstable air masses,  
13 moist low-level jets, steep orography and a slow evolving synoptic pattern) for severe  
14 rainfall processes on complex orography. For the two Ligurian events, this role has been  
15 analyzed through the available observations (e.g. Meteosat Second Generation - MSG,  
16 Moderate Resolution Imaging Spectroradiometer, the Italian Radar Network mosaic and  
17 the Italian Raingauge Network observations).

18 We then address the possible role of the sea-atmosphere interactions and propose  
19 a characterization of these events in terms of their predictability.

20

## 1 **1 Introduction**

2 The Mediterranean coastal cities, both on southern and northern sides, are used to flood  
3 and flash-floods. The Mediterranean Sea acts as a large heat and moisture reservoir and  
4 source from which convective and baroclinic atmospheric systems get part of their  
5 energy. The interaction between convective processes originating on the warm sea and  
6 sudden orographic lifting very close to the coast produces heavy rainfalls. It often  
7 happens that the rain accumulated in one hour accounts for the entire monthly average for  
8 that location, and the rain accumulated in one day can account for the entire yearly  
9 average (Altinbilek et al. 1997). The morphology of the Mediterranean basin with  
10 numerous small and steep river catchments can turn the intense precipitation into severe  
11 devastating flash-floods and floods. Large scale environment propitious to heavy  
12 precipitation is relatively well known. However progress has to be made on the  
13 understanding of the mechanisms that govern the precise location of the precipitation  
14 system as well as of those that can occasionally produce uncommon amounts of  
15 precipitation (Ricard et al. 2012).

16 To mention a few of these disastrous events we should recall, for example, the flooding  
17 of Genoa city - northern Italy- in 1970 (Roth 1996, Siccardi 1996), the Vaison-la-  
18 Romaine – southern France – in 1992 (Massacand et al. 1998 and Ducrocq et al. 2008),  
19 the Izmir case - west Turkey- in 1995 (Komoscu et al. 1998), and the most catastrophic  
20 flash flood of Algiers in 2001. Each event hit very small-size catchments (10-50 km<sup>2</sup>),  
21 leaving unaffected nearby basins, thus exhibiting a very fine-grained structure of the  
22 rainfall precipitation field. They produced many casualties: in particular the last one  
23 produced a very large number of victims, on the order of seven hundred, in the Bab el  
24 Oued borough of Algiers. The spatio-temporal evolution of the Algiers event was

1 discussed by a number of papers (Argence et al. 2008, Brancovic et al. 2008 and Tripoli  
2 et al. 2005): the apparent predictability of the Algiers event suggested a controlling role  
3 by large-scale forcing. In fact the European Centre for Medium-Range Weather Forecast  
4 model (IFS model version 23r4, with a horizontal spacing of  $1.8^\circ$  - about 200 km  
5 resolution – and 40 sigma levels in the vertical) detected the structure of the cyclogenesis  
6 of the event. Furthermore the Office National de la Meteorologie of Algeria issued a  
7 flood forecast as early as 5 November 2001. The flooding took place between 9 and 10  
8 November: it was a flash flood phenomenon on a very small creek (about  $15 \text{ km}^2$ )  
9 flowing through the Kasbah city center. In the same period the total rain depth observed at  
10 a rain gauge 18 km away was negligible. The closer examination introduced numerically  
11 by Tripoli et al. (2005) revealed that significant mesoscale development led to the actual  
12 weather pattern over the city. Wind Induced Surface Heat Exchange (WISHE, Emanuel  
13 1994) over the warm waters north of Tunisia and Libya raised the Planetary Boundary  
14 Layer (PBL) humidity and temperature until matched potential temperature values and  
15 therefore the resulting reduction of the Level of Free Convection (LFC) triggered deep  
16 moist convective processes. The rainfall amount was estimated up to 250mm in 48 h.  
17 The characteristics of the events that hit the small catchments of Liguria in October and  
18 November 2011 seem very similar to the historical ones mentioned above, in terms of  
19 dynamics and thermodynamics forcings, as well as from a hydrological impacts  
20 standpoint. The difference is that for the recent Liguria events the rainfall measurements  
21 at the surface were very dense, and meteorological radar and satellite observations were  
22 available as well, whilst little more than numerical modeling results could be used to  
23 explain the fine-grained structure of the rainfall field of the previously mentioned

1 historical events. This is the reason why we devoted this paper to the description of the  
2 available observations of the recent Liguria events: in these cases the physical hypotheses  
3 about the development of the events can be validated, at least partially, based on the  
4 available observations.

5 The first flash-flood took place on 25 October, hereinafter we will refer to OCT25 to  
6 indicate this event. An anomalous intense rainstorm ripped through the region and  
7 inflicted serious damage on the Cinque Terre coastal towns of Monterosso and Vernazza,  
8 on eastern Liguria complex orography area (Figure 1, lower right). The Brugnato  
9 raingauge station, in the center of the event (10 km from the coast over a 500 m hill)  
10 registered up to 470 mm of rain in 6 hours – a third of the average annual rainfall, with a  
11 peak of 150 mm in one hour. Thirteen people lost their life.

12 Nine days later, on 4 November, the city of Genoa, the capital of the Liguria region,  
13 located at the meridional edge of the local Appennines range (Figure 1, lower left) was  
14 gutted by a torrential rainfall event with up to 450 millimetres (7 km from the coast over  
15 a 300 m hill) of rain in 5 hours. Six people were killed. Hereinafter we will refer to  
16 NOV4 to indicate this event.

17 The large-scale features of these events were well predicted by the Liguria region meteo-  
18 hydrological Center (Silvestro et al. 2012).

19 The goal of this paper is to gain a deeper understanding of these events according to the  
20 works of Doswell et al. (1996), Miglietta and Rotunno (2010), Romero et al. (2000),  
21 Rotunno and Ferretti (2001), and Yu et al. (2007) all together converging on these key  
22 ingredients for severe flood events on complex orography: i) conditional or potential  
23 unstable air masses; ii) moist low-level jets that impinge the first foothills; iii) steep

1 orography which helps to release the conditional instability associated with the low-level  
2 jet; and iv) a slow evolving synoptic pattern that slows down the advance of the heavy  
3 precipitation system, hence increasing their persistency, or maintains the same favourable  
4 environment for heavy precipitation.

5 Section 2 is devoted to characterize both events at the synoptic scale; to understand the  
6 mesoscale forcings through the use of remote sensing observational datasets (Meteosat  
7 Second Generation - MSG, Moderate Resolution Imaging Spectroradiometer and Italian  
8 Radar Networkmosaic); to analyze the rainfall patterns, and to address the possible role  
9 of the sea-atmosphere interactions.

10 Section 3 focuses on the characterization of the predictability of the two events, based on  
11 the approach of Molini et al. (2011). Section 4 presents final discussion and conclusions.

## 12 **2 October 25<sup>th</sup> event**

### 13 **2.1 Synoptic scale**

14 The severe weather event that struck eastern Liguria on October 25<sup>th</sup> was associated to a  
15 large depression positioned off Ireland's western shore since the day before. A deep  
16 trough extending almost from the arctic circle to northern Africa entered the  
17 Mediterranean late on October 24<sup>th</sup>, whilst a high pressure system (1035 mbar) was  
18 between north-eastern Europe and the southern Balkans, with a maximum near the Baltic  
19 countries, not allowing the cyclonic structure to move eastwards (Figure 2a, ingredient  
20 iv).

21 Early on October 25<sup>th</sup> a cold front was evident on the western Mediterranean, as depicted  
22 by the airmass RGB (Figure 2b), which is a combination of data from SEVIRI WV6.2,  
23 WV7.3, IR9.7 and IR10.8 channels and thus usable day and night (Lensky et al., 2008).

1 This synoptic configuration stimulated the second ingredient of mid-latitude  
2 meteorological extremes, i.e., intensive advection of warm and moist air of sub-tropical  
3 origin on the Ligurian sea area (Figure 2c, ingredient ii), inducing two different weather  
4 regimes over western and eastern Liguria. Western Liguria was mainly affected by a  
5 widespread and stratiform precipitation, while deep moist convection played the main  
6 role in eastern Liguria . Thus, the atmospheric scenario saw a southwesterly flow on the  
7 storm's right wing (warm front) channeled between Italy and the Sardinia/Corsica east  
8 coasts and moistened by the warm Mediterranean water that began to bring a significant  
9 amount of water vapor on eastern Liguria (Figure 2c).

10 Radiosoundings data shown in Figure 2 (Barcelona, Palma de Mallorca, Nimes, Pratica di  
11 Mare, Ajaccio and Milan) provide a quantification of the thermodynamical atmospheric  
12 structure on November 4<sup>th</sup> at 00UTC. All the stations are located in the western  
13 Mediterranean, appreciably near to the places where the severe event occurred. Relative  
14 humidity values in the lower troposphere were around 70% and temperature gradient  
15 around 6K/1000 m, hence confirming the presence of potentially instable air masses  
16 (ingredient i) during OCT25.

17 In the meantime, a vigorous north wind blowing across the central ligurian Apennines  
18 prompted by the high pressure on the Adriatic sea (ingredient iv), stuck the moist flow  
19 over eastern Liguria for almost the whole day and promoted a local uplift supportive for  
20 flash-flood storms: the resulting prominent convergence line (Wang et al. 2000) on the  
21 eastern portion of the Genoa sea is depicted by the ASCAT image (Figure 4) by a solid  
22 red curve. Coastal wind stations (Table 1) on the line left side showed wind blowing from



1 N-NW (15-20 km/h), while stations on its right measure wind from S-SE and speed  
2 around 15-20 km/h.

### 3 **2.2 Mesoscale**

4 At the mesoscale, local steep topography (ingredient iii) was the trigger to the onset of an  
5 organized and self-regenerating mesoscale convective system (MCS) that poured severe  
6 rainfall on Cinque Terre, Brugnato (Vara river) and later on Magra river. Sudden rainfall  
7 amounts reached 160mm/h, 350/3h and 450/6h. Several landslides, mudslides and debris  
8 flows together with flash floods affected the small catchments in this area.

9 The C-band, dual polarization radar of Mt. Settepani (located on the Appennine ridge  
10 approximately 100 km south-west from the area of interest) allows to gain a deeper  
11 understanding of the MCS morphology (Figure 5): the vertical cross-sections clearly  
12 show the slantwise organization of the system with its upwind coastal portion mainly  
13 associated to warm rain processes (zero isotherm around 4000 m), while the horizontal  
14 view depicts the observed V-shaped precipitation system with well-defined boundaries  
15 and highly persistent localization, as suggested by the map in Figure 6, which highlights  
16 the period of time (between 8:00 UTC and 15:00 UTC) where reflectivity was above a 40  
17 dB threshold.

18 The V-shaped structure is also evident in the enhanced IR10.8 MSG image on October  
19 25<sup>th</sup> at 12 UTC (Figure 7a). This product is used in combination with the severe storm  
20 RGB (Figure 7b) to refine the overshooting top characteristics by cloud top microphysics:  
21 in this case the continental top cloud appears to be thick and composed of small ice  
22 particles. This inference is confirmed by another MSG product, Cloud Top Temperature  
23 and Height (CTTH, Figure 7c). The CTTH product confirms the slantwise structure of the

1 V-shaped convective cell, with cloud top heights ranging from 4000-5000 m in the  
2 Liguria sea portion of the structure up to 15000 m over the continental part.

### 3 **2.3 Precipitation analysis**

4 OCT25, mainly affecting Brugnato-Borghetto and Cinque Terre (Figure 8), was observed  
5 by the remotely automated weather stations network operated by the National Civil  
6 Protection Department. Between 8 UTC and 15 UTC, rainfall accumulation reached 500  
7 mm in the areas that were hit most severely. The radar derived rainfall map shows very  
8 pronounced spatial variability of the rainfall processes (Figure 10). As Figure 8 shows,  
9 Serò di Zignago and Santa Margherita Vara are two villages located about 4 and 6 km  
10 respectively from the small town of Brugnato in the Vara Valley: Vara is a left-bank  
11 tributary to the Magra river and drains an area slightly bigger than 1700km<sup>2</sup> with a  
12 hydrological concentration time ( $T_c$ ) around 6 hour.

13 The comparison of the raingauges at these three adjacent locations shows large  
14 differences in the hyetographs, confirming the very localized features of the auto-  
15 regenerating thunderstorm responsible for this event (Figure 9). There is a factor 3  
16 between Brugnato's raingauge and Serò di Zignago (S.ta Margherita Vara) for  $d=1$ hour  
17 and  $d=3$  hours. Differences smoothen as longer durations are analyzed, yet the ratio stays  
18 over 1.7 (Table 2) even for  $d=24$  hours.

19 Conversely, rainfall hit with approximately the same strength Monterosso and Vernazza,  
20 two coastal villages separated by more than 10 km from Brugnato. The reason has to be  
21 found in their position, since they are both aligned along the main direction of the south-  
22 westerly moist air jet that fed the thunderstorm triggered by coastal topography, and they

1 experienced a very similar total amount of rainfall as well as Brugnato, as the radar  
2 derived rainfall map also suggests (Figure 10).

### 3 **3 November 4<sup>th</sup> event**

#### 4 **3.1 Synoptic scale**

5 The heavy rainfall episode that provoked the deadly flooding in Genoa was the most  
6 powerful outburst within the larger system that affected southern Europe November 3<sup>rd</sup> to  
7 8<sup>th</sup>. The extra tropical macro-storm originated from the extension of the 2011 Halloween  
8 Nor'easter (Ryan, 2011) that brought early heavy snowfall on central and eastern US in  
9 the last October day. This system, coming across the Atlantic Ocean, regained strength by  
10 combining with the remnants of tropical storm Rina (October 23<sup>rd</sup>-28<sup>th</sup>, Yucatan and  
11 Cuba), which enhanced significantly its precipitable water content.

12 The developing of severe rainfall was the result of the complex combination the  
13 aforementioned meteorological ingredients for flash floods. Figure 11a presents the 500-  
14 hPa height analysis at 00 UTC on NOV4, just a few hours in advance of the beginning of  
15 the precipitation period over Liguria. An upper-level cold low centered north-west of  
16 Ireland and extended southbound to the Iberian Peninsula (Figure 11b), resulted in  
17 diffluent southwesterly flow over the Ligurian Appenines ridge at 500 hPa, while the  
18 main flux at lower altitude was southeasterly. At the same time, a strong pressure ridge  
19 centred on Ukraine and the eastern Balkans acted as a block to the eastward motion of the  
20 cyclonic structure (ingredient iv).

21 This synoptic pattern result in the onset of an intense south-south-eastern and very moist  
22 flow (Figure 11c, ingredient ii) which triggered, together with the local topography  
23 (ingredient iii), a series of severe rainfall episodes beginning on November 3<sup>rd</sup> late in the

1 afternoon (south-eastern France). In the early morning of November 4<sup>th</sup>, Genoa's western  
2 boroughs were hit by a series of organized self-regenerating thundercells caused by the  
3 convergence of the moist flow on a pretty small area (less than 10 km<sup>2</sup>). The  
4 hypothesized presence of Doswell's ingredient i) is supported by skew-T diagrams of six  
5 radiosonde sounding stations (Barcelona, Palma de Mallorca, Nimes, Pratica di Mare,  
6 Ajaccio and Milan; Figure 11) located under or near the frontal system at 00 UTC 4  
7 November 2011: relative humidity values are around 70-75% in the lower troposphere,  
8 and temperature gradient around 6 K/1000 m.

### 9 **3.2 Mesoscale**

10 As in the case of the OCT25, also NOV4 was associated at the mesoscale with a V-  
11 shaped, isolated and self-regenerating convective cell triggered in the Gulf of Genoa  
12 during the night of November 4<sup>th</sup> (1-2UTC). The cell was again produced by the  
13 interaction of cold air coming from north-northwest in the central-western part of the  
14 Gulf of Genoa, with warm and moist air coming from southeast into the same region,  
15 resulting again into a mechanism of cold pool-shear interaction (Moncrieff and Changai,  
16 1999), driven by local convergence at low-level-flow separation lines (Wang et al.,  
17 2000), well depicted by the ASCAT image (Figure 13). As in OCT25, coastal wind  
18 stations on the left side of the convergence line showed wind blowing from N-NW (15-20  
19 km/h), while stations on its right measure wind from S-SE and speed around 15-20 km/h.  
20 The Italian Radar Network observed the structure but unfortunately the closest radar  
21 located at Mt. Settepani, in Liguria, was not running due to technical problems. The radar  
22 that actually observed the structure is located near Turin (Bric della Croce - ARPA  
23 Regione Piemonte), more than 100 km from the center of the storm. The low quality of

1 the observation is mainly due to the long distance combined with attenuation and  
2 orographic beam blocking. The reflectivity pattern over the city of Genoa suffered strong  
3 attenuation, but it is nevertheless possible to quantify its persistence: Figure 14 shows a  
4 structure persistence over Genoa city basins (Bisagno and Rio Fereggiano) weaker than  
5 that exhibited by the October 25<sup>th</sup> cell. This cell started wandering along the eastern coast  
6 (from 3:00 to 9:00 UTC) of Liguria and finally was stuck over the western portion of  
7 Genoa hills (Figure 15a) generating the dramatic flash flood of the Rio Fereggiano. Once  
8 again, the very high rainfall depth is associated with a slantwise structure with the cloud  
9 top continental portion appearing to be thick, composed of small ice particles (Figure  
10 15b), while the upwind one is dominated by warm rain processes, as for the October 25<sup>th</sup>  
11 event. When compared with the convective structure responsible for the October 25<sup>th</sup>  
12 event, this self-regenerating convective cell appears to be less developed vertically  
13 (11000-12000 m) and less coherent (Figure 15c).

### 14 **3.3 Precipitation analysis**

15 The precipitation analysis of this event relies on Liguria's National Civil Protection  
16 Department raingauge network, named OMIRL (Liguria Region Hydro-Meteorological  
17 Observatory), and on real-time semi-professional stations, belonging to the LIMET  
18 (Liguria Meteorological) association: the total number of sensors is about 200, with an  
19 average regional density of about  $1/40\text{km}^2$ . The most severe rainfall hit Genoa's mid-  
20 eastern part and in particular the borough of Quezzi, which is a densely populated  
21 borough built on the left bank of the Bisagno creek, a small catchment that drains a total  
22 area of  $90\text{ km}^2$  (Figure 16). One of its inlets, Rio Fereggiano ( $5\text{ km}^2$  area), crosses Quezzi  
23 and its flood was responsible for 6 casualties. Two raingauges are here considered

1 (Figure 17): one belonging to LIMET network and located on the Rio Fereggiano, and the  
2 other belonging to OMIRL official network, located 2 km away on the Bisagno.  
3 The sensors provide further proof of the localization of the severe rainfall (Figure 17),  
4 already discussed in Figure 14: despite their proximity, these two sensors observed quite  
5 dissimilar rainfall amounts. Differences are displayed in Table 3. LIMET exceeds  
6 OMIRL by almost 30%. The return period of the event evaluated with the OMIRL  
7 observations is in the order of 50 years whilst the return period of the event with LIMET  
8 observations exceeds 200 years, as computed by means of the TCEV (Two Components  
9 Extreme Value Distribution) and for a level of confidence  $\alpha = 0.05$  (Boni et al. 2006).  
10 Raingauges 5-10 km away observed nearly no rain.

#### 11 **4 October 25<sup>th</sup> event and November 4<sup>th</sup> event: sea surface temperature** 12 **role**

13 While the role of tropical north Atlantic Sea Surface Temperature (SST) in driving  
14 tropical storm activity has been discussed and assessed extensively in the literature  
15 (Landsea 1996, Trenberth 2005), a similar potential role has not been explored in detail in  
16 the case of mid-latitude storms over the Mediterranean area. It is however well  
17 understood that a warmer SST increases air-sea surface heat fluxes which in turn moisten  
18 and destabilize the marine atmospheric boundary layer, resulting in an increase of the  
19 available energy and moisture for atmospheric convection and thus precipitation.

20 In this context, an SST analysis is undertaken to gain a deeper understanding of the  
21 spatio-temporal properties of these events and the possible role of sea-atmosphere  
22 interactions in triggering and driving torrential events.

23 The OCT25 SST Anomaly scenario is shown in Figure 18. The left panel shows the  
24 G1SST (Global 1-km Sea Surface Temperature) product (Chao et al., 2009) produced

1 daily by the Jet Propulsion Laboratory Regional Ocean Modeling System (JPL-ROMS)  
2 group<sup>1</sup> while the right panel displays the Italian Research Council - Mediterranean Sea  
3 Surface Temperature L4 (CNR-MED SST L4) produced and distributed in near-real time,  
4 in the framework of the GMES MyOcean<sup>2</sup> project, by the Institute of Atmospheric  
5 Sciences and Climate - Satellite Oceanography Group (ISAC-GOS).

6 Both anomaly products are computed using the CNR daily pentad mean climatology sea  
7 surface temperature, which is based on the AVHRR PATHFINDER v5 data set over the  
8 1985-2004 time period (Marullo et al. 2007).

9 Although the use of these products is limited by the lack of input SST data from  
10 microwave sensors when the cloud cover is significant, they are a useful tool for a  
11 qualitative description of a very likely SST Anomaly (SSTA) scenario.

12 Both panels show a positive anomaly of temperature in the central part of the Ligurian  
13 sea: certainly the two datasets give different SSTA patterns, that can be attributed to  
14 different data fusion techniques adopted (Chao et al. 2009 and Buongiorno Nardelli et al.  
15 2012), and to the fact that for G1SST over the Mediterranean sea the IMAGER/GOES  
16 observational data are not available. However for both of them a major anticyclonic eddy  
17 structure and several minor structures distributed in the central part of the basin are  
18 evident.

19 Figure 18 also shows a map of SST anomaly overlaid with the footprint of the radar-  
20 derived rainfall accumulation map.

21 The main positive SST anomaly located in the northeastern part of the basin, from which  
22 the flash-flood producing storm seems to have originated, broadened both in north-

---

<sup>1</sup><http://ouocean.jpl.nasa.gov/SST/#>

<sup>2</sup><http://www.myocean.eu.org/>

1 southand east-west directions as it approached the coast ( Figure 18), and possibly fed the  
2 storm according to the WISHE mechanism (see section 3).  
3 Along the same lines, the maps of SST anomaly for NOV4 are shown in Figure 19: a  
4 positive temperature anomaly in the central part of the Ligurian basin is evident in both  
5 figures with several structures characterized by positive values distributed in the central  
6 part of the basin, from which the finger-convection responsible for NOV4 seems to  
7 originate. The link between anomaly and rainfall origin is still present, but it appears  
8 somewhat weaker than for OCT25. We must recall that the radar of the Italian Radar  
9 Network closest to the precipitation field was only partly operational during the first part  
10 of this event. For this reason, the rainfall pattern was very likely underestimated and the  
11 localization of its starting point is more uncertain than in the previous case.

## 12 **5 October 25<sup>th</sup> event and November 4<sup>th</sup> event: predictability analysis**

13  
14 Mid-latitude severe events affecting Mediterranean regions can be classified into two  
15 categories (Molini et al. , 2009): events mainly long-lived (lifetime >12hours) and  
16 widespread (area>50x50km<sup>2</sup>, hereinafter referred to as T1), and events characterized by  
17 smaller space-time extent (hereinafter T2). A quasi-equilibrium environment is a  
18 common feature for T1 events, while in general localized and intense storms belong to  
19 the T2 group (Molini et al., 2010).

20 Differences between the two groups are found not only in their spatio-temporal length  
21 scales but also on the role that large- or local-scale forcing play on their outbreak, which  
22 can be determined by considering the convective heating time scale  $\tau_{CH}$ . This timescale  
23 provides a measure of the rate at which Convective Available Potential Energy (CAPE) is  
24 consumed by convective heating. Usually mid-latitude severe events are triggered in a



1 quasi-equilibrium environment (Emanuel 1994 and 2000). This means that the CAPE  
 2 growth rate due to large scale forcing almost balances its consumption by local  
 3 convection: in this case, convective timescales  $\tau_{CH}$  are typically small compared to  
 4 timescales of forcing changes, thus large scale forcing determines the statistical  
 5 properties of convection and the spatio-temporal behavior of the corresponding severe  
 6 rainfall events, making them more predictable (Done et al. 2006 and Molini et al. 2010).  
 7 On the contrary a non-equilibrium environment requires heavy rainfall to originate from a  
 8 weaker synoptic forcing. Therefore in a non-equilibrium case, convection is controlled by  
 9 local modalities of triggering, e.g. the existence of a strong convective inhibition  
 10 condition, thus with a low degree of predictability.

11 Done et al. (2006) describes how to calculate  $\tau_{CH}$  from raindepths and CAPE, according  
 12 to the following formula:

$$\tau_c = \frac{CAPE}{\frac{dCAPE}{dt}}$$

13 with

$$\frac{dCAPE}{dt} = \frac{1}{3600} \frac{i_R L_V g}{c_p T_0 \rho_0}$$

14 where  $i_R$  is the rainfall intensity ( $\text{mm h}^{-1}$ ),  $L_V$  the latent heat of vaporization,  $g$  the  
 15 acceleration due to gravity,  $c_p$  the specific heat of air at constant pressure and  $T_0$  and  $\rho_0$   
 16 reference values of temperature and density, respectively.

17 Molini et al. (2010) found that quasi-equilibrium environments typically show  $\tau_{CH}$   
 18 smaller than 6 hours, whilst values larger than that characterize non-equilibrium  
 19 configurations. Done et al. (2006) argue that a typical synoptic time-scale would be a day  
 20 or more. Overland, changes in forcing associated with the diurnal cycle are likely to be

1 relevant, so a shorter threshold time-scale of around 6 h is adopted (Done et al. 2006,  
2 Molini et al. 2010).

3 Hourly  $\tau_{CH}$  calculations were carried out using the hourly raindepth provided by the  
4 Italian National Civil Protection real-time raingauges network, and 3-hourly CAPE  
5 estimates at  $0.7^\circ$  horizontal resolution retrieved from the ERA Interim database, the latest  
6 ECMWF global atmospheric reanalyses available for the period 1989-present (Simmons  
7 et al. 2007). The 3-hourly CAPE field was linearly interpolated in space and time to  
8 match the geographical coordinates of the raingauges that actually observed the event and  
9 their hourly sampling.

10 The  $\tau_{CH}$  values for NOV4 stay small during its most intense phase (from 9 am to 1 pm;  
11 Figure 20, lower panel); they indicate this event to be a T1. The increase in the last part is  
12 due to the rainfall on the leeward side of the Apennines ridge, loosely related to the event that  
13 hit the city in the morning. OCT25 is as well a T1 event (Figure 20, upper panel). Heavy  
14 rainfall started around 9UTC morning whilst the observed maxima were observed  
15 between 13 and 14UTC (at the Cinque Terre and Brugnato stations).

16 The T1 classification of OCT25 and NOV4 is also supportive of the importance of the  
17 SSTA for these events and thus of their feeding according to a WISHE mechanism: since  
18 WISHE involves a positive feedback between the circulation and heat fluxes from the sea  
19 surface, with stronger circulation giving rise to larger surface fluxes of heat, which are  
20 then quickly redistributed aloft by convection, in turn strengthening the circulation. Then  
21 this emphasises the role of the surface fluxes as the principal rate-limiting process, while  
22 convection serves only to redistribute heat, this corresponding to the quasi-equilibrium  
23 vision for OCT25 and NOV4.

## 1 **6 Discussion and conclusions**

2 OCT25 and NOV4 show similarities from several points of view.

3 Both are characterized by a pretty short duration (approximately 6 hours in their most  
4 intense part) and in both cases the total rainfall amount significantly exceeds the value of  
5 multi-centennial return period (Boni et al. 2006).

6 The large-scale features of the two can be assumed to be analogous: a depressionary  
7 system originated on the western Atlantic and broke into the Mediterranean to find a  
8 robust block exerted by a stationary high pressure structure located over eastern Europe.

9 In both events the creation of positive vertical vorticity in the low and mid troposphere by  
10 the wind-shear is clear from the synoptic maps (reanalyses from NOAA/NCEP Model  
11 corresponding to 12UTC of corresponding days) at different levels shown in Figure 21.

12 The surface wind direction over Liguria on October 25<sup>th</sup> (November 4<sup>th</sup>) was from the  
13 SSW (S), while at mid-levels it was from the WSW (SW); in either situation and in a  
14 similar fashion, therefore, we note the very moist air flux towards land, and how it rotates  
15 clock-wise and notably intensifies with height in the low to middle layers of atmosphere.

16 The effect of such a configuration contributed to the long persistence of auto-regenerating  
17 V-shaped heavy rainfall structures over small areas, smaller than  $50 \times 50 \text{ km}^2$  which in turn  
18 were responsible for flash floods that affected small and medium-sized catchments.

19 Following these considerations, large-scale forcing played a leading role in provoking  
20 heavy rains. The consequent quasi-equilibrium configuration is confirmed by the analysis  
21 of the convective timescale: in both cases the value of  $\tau_{CH}$  stays below the threshold of 6  
22 hours for most of the event as the production of CAPE by large-scale processes is nearly  
23 balanced by its consumption by convective phenomena, and thus CAPE values stay

1 small. Moreover low values of CAPE were measured by numerous radiosoundings of the  
2 nearby stations.

3 The local factor which, together with the strong south-westerly (south-easterly)  
4 circulation, triggered precipitation was represented for the October 25<sup>th</sup> (November 4<sup>th</sup>)  
5 study case by the steep coastal topography which compelled moist air to rise suddenly  
6 and then condensate into rain, i.e. the well-known orographic lifting mechanism that  
7 usually causes flash-floods in Italian shoreline towns and in the nearby inland boroughs.  
8 Miglietta and Rotunno (2009) developed a conceptual model for large convective  
9 orographic rainfall based on three non-dimensional numbers: the ratio of mountain height  
10 to the level of free convection  $h_m/LFC$ , the slope parameter  $h_m/a$  (with  $a$  ridge half-width),  
11 and the third is the ratio of an advective timescale  $\tau_a = a/U$  to a convective growth  
12 timescale  $\tau_c = h_t/(CAPE)^{1/2}$  (the time that convective elements take to grow, covering the  
13 tropopause height  $h_t$  and producing rain at the surface). For the two Liguria events, the  
14 following scales can be estimated:  $h_m \approx 500$  m,  $LFC \approx 1000$  m (estimated using Lawrence  
15 2005),  $a \approx 10000$  m,  $U \approx 8$  m/s (from Advanced Scatterometer, ASCAT, data products),  
16  $h_t \approx 10000$  m (average value for OCT25 and NOV4 from CTTH product), and  $CAPE \approx$   
17  $500$  J/kg (from ERA-Interim reanalysis). Consequently, both events respect the pre-  
18 requisites for large convective orographic rainfall:

- 19 •  $\tau_a / \tau_c \approx 3.0$
- 20 •  $h_m / LFC \approx 0.5$
- 21 •  $h_m / a \approx 0.05$

1 corresponding to a regime where the orographic trigger is significant and the peak is  
2 located near the top of the ridge (see figure 2 in Miglietta and Rotunno 2010), as indeed  
3 observed for both events.

4 Another very interesting aspect deals with the measure of sea surface temperature and  
5 especially its anomaly with respect to climatological values. In particular, the sea surface  
6 positive anomaly is a concomitant factor which possibly contributes to the exceptional  
7 severity of the rainfall processes, according to the WISHE mechanism. Furthermore, in  
8 both cases, if SSTA patterns and the radar-derived rainfall accumulation map are  
9 overlaid, there are considerable similarities: V-shaped precipitation patterns seem to  
10 spread out from the higher anomalies sectors. This feature is more evident for the October  
11 25<sup>th</sup> study case since radar products did not suffer any gap in the timeseries as  
12 unfortunately happened during November 4<sup>th</sup>.

13 Some studies discuss the effect of SST on torrential Mediterranean rain events (Pastor et  
14 al 2001, Lebeaupin et al. 2006). These studies state that SST plays a key role in the  
15 recharge of moisture and heat and contributes to increased conditional convective  
16 instability. However this fact remains to be verified and further research is needed for  
17 fully defining the role of SST in controlling Ligurian intense events. For the two Ligurian  
18 events here presented, it is planned to run high resolution numerical models to clarify  
19 whether the presence of a positive anomaly of sea surface temperature can be a factor  
20 which is significant in the process of triggering and driving Ligurian torrential events.

21 Future work will be devoted to undertaking a modelling study of the November 4<sup>th</sup> event  
22 to gain a deeper understanding of the physical processes associated with these prototypal  
23 Mediterranean storm events.

1 *Acknowledgments.*

2 This work is supported by Italian Civil Protection Department and by Regione Liguria.

3 We acknowledge Regione Liguria and Regione Piemonte for providing us with the data

4 of the regional meteorological observation networks. We acknowledge the Italian Civil

5 Protection Department for providing us with the Italian Radar Network data. We

6 acknowledge the LIMET association for providing us with the data from their

7 meteorological observation network. We acknowledge the Institute of Atmospheric

8 Sciences and Climate - Satellite Oceanography Group (ISAC-GOS) for providing us with

9 the CNR-MED Sea Surface Temperature data. We are very grateful to the meteorologists

10 and the hydrologists of the Meteo-Hydrologic Centre of Liguria Region, for many useful

11 discussions. The portion of work carried out by Simone Tanelli was performed at Jet

12 Propulsion Laboratory, California Institute of Technology, under contract with National

13 Aeronautics and Space Administration, support from the Precipitation Measurement

14 Missions program is gratefully acknowledged. Nicola Rebola and Antonio Parodi would

15 like to acknowledge the support by the FP7 DRIHM (Distributed Research Infrastructure

16 for Hydro-Meteorology, 2011-2015) project (contract number 283568). The authors

17 thanks also Garvin Cummings for the help in revising this paper.

18

19

## 1 **References**

- 2 Altinbilek D., E. C. Barret, T. Oweis, E. Salameh, and Siccardi F,1997: Rainfall  
3 Climatology on the Mediterranean, EU-AVI 080 Project ACROSS – Analyzed  
4 Climatology Rainfall Obtained from Satellite and Surface data in the Mediterranean  
5 basin. *EC reports*..
- 6 Chao, Y., Z. Li, J. D. Farrara, and P. Huang,2009: Blended sea surface temperatures from  
7 multiple satellites and in-situ observations for coastal oceans. *J. Atmos. Oceanic*  
8 *Technol.*, **26** (7), 1435-1446, 10.1175/2009JTECHO592.1.
- 9 Argence, S., D. Lambert, E. Richard, J.P. Chaboureau, and N. Söhne, 2008: Impact of  
10 initial condition uncertainties on the predictability of heavy rainfall in the Mediterranean:  
11 a case study. *Quart. J. Roy. Meteor. Soc.*,**134** (636), 1775-1788.
- 12 Boni, G., A. Parodi, and R. Rudari, 2006: Extreme rainfall events: learning from rain  
13 gauge time series, *Journal of Hydrology*, **327**, 304–314,  
14 doi:10.1016/j.jhydrol.2005.11.050.
- 15 Branković, Č., B. Matjačić, S.Ivatek-Šahdan, and R. Buizza, 2008: Downscaling of  
16 ECMWF Ensemble Forecasts for Cases of Severe Weather: Ensemble Statistics and  
17 Cluster Analysis. *Monthly Weather Review*,**136**(9), 3323-3342.
- 18 Buongiorno Nardelli B., C. Tronconi, R. Santoleri, 2013: High and Ultra-High resolution  
19 processing of satellite Sea Surface Temperature data over the Southern European Seas in  
20 the framework of MyOcean project, *Rem. Sens. Env*, **129**, 1-16, doi:  
21 10.1016/j.rse.2012.10.012.
- 22 Delrieu, G., V. Ducrocq, E. Gaume, J. Nicol, O. Payrastre, E. Yates, P.-E. Kirstetter, H.  
23 Andrieu, P. A. Aral, C. Bouvier, J. D. Creutin, M. Livet, A. Anquetin, M. Lang, L.  
24 Neppel, C. Obled, J. Parent-du-Chatelet, G. M. Saulnier, A. Walpersdorf, and W.  
25 Wobrock, 2005: The catastrophic flash-flood event of 8-9 September 2002 in the Gard  
26 region, France: a first case study for the Cévennes-Vivarais Mediterranean Hydro-  
27 meteorological Observatory. *J. Hydrometeorology*, **6**, 34-52.
- 28 Done J.M., G.C. Craig, S.L. Gray, P.A. Clark, and M.E.B. Gray, 2006: Mesoscale  
29 simulations of organized convection: importance of convective equilibrium. *Quart. J.*  
30 *Roy. Meteor. Soc.* **132**, 737–756.
- 31 Doswell, C.A., H.E. Brooks, and R.A. Maddox, 1996: Flash Flood Forecasting: An  
32 Ingredients-Based Methodology. *Wea. Forecasting*, **11**, 560–581. doi:  
33 [http://dx.doi.org/10.1175/1520-0434\(1996\)011<0560:FFFAIB>2.0.CO;2](http://dx.doi.org/10.1175/1520-0434(1996)011<0560:FFFAIB>2.0.CO;2).
- 34 Ducrocq, V., O. Nuissier, D. Ricard, C. Lebeau-pin, and T. Thouvenin, 2008: A numerical  
35 study of three catastrophic precipitating events over western mediterranean region  
36 (Southern France): Part II: Mesoscale triggering ans stationarity factors. *Quart. J. Roy.*  
37 *Meteor. Soc.*, **134** (630), 131–145
- 38 Emanuel K.A, 1994.:Atmospheric Convection. Oxford University Press,580 pp.
- 39 EmanuelK.A., 2000:. Quasi-equilibrium thinking. General Circulation Model  
40 Development. D. A. Randall, Ed. Academic Press, 225–255.

- 1 Komuscu, A.U., A. Erkan, and S. Celik, 1998: Analysis of the Meteorological and  
2 Terrain Features Leading to the Izmir Flash Flood, *Natural Hazards*,**18**,1-25.
- 3 Landsea, C. W., R. A. Pielke Jr., A. M. Mestas-Nunez, and J. A. Knaff, 1999: Atlantic  
4 basin hurricanes: Indices of climatic changes. *Climatic Change*,**42**, 89–129.
- 5 Lawrence, M. G., 2005: The Relationship between Relative Humidity and the Dewpoint  
6 Temperature in Moist Air: A Simple Conversion and Applications. *Bull. Amer. Meteor.*  
7 *Soc.*, **86**, 225–233.
- 8 Lebeau-pin, C., V. Ducrocq, and H. Giordani,2006: Sensitivity of torrential rain events to  
9 the sea surface temperature based on high-resolution numerical forecasts, *J. Geophys.*  
10 *Res.*, **111**, D12110, doi:10.1029/2005JD006541.
- 11 Lensky, I. M., and D. Rosenfeld: Clouds-Aerosols-Precipitation Satellite Analysis Tool  
12 (CAPSAT). *Atmos. Chem. Phys.*, **8**, 6739–6753, 2008.
- 13 Marullo, S., BB. Nardelli, M. Guarracino, and R. Santoleri, 2007: Observing the  
14 Mediterranean Sea from space: 21 years of Pathfinder-AVHRR sea surface temperatures  
15 (1985 to 2005): re-analysis and validation. *Ocean Sci.*, **3**, 299–310.
- 16 Massacand, A. C., H. Wernli, and H. C. Davies,1998: Heavy precipitation on the alpine  
17 southside: An upper- level precursor, *Geophys. Res. Lett.*, **25(9)**, 1435–1438,  
18 doi:10.1029/98GL50869.
- 19 Miglietta, M. M., and R. Rotunno, 2009: Numerical simulations of conditionally unstable  
20 flows over a ridge. *J. Atmos. Sci.*, **66**, 1865-1885.
- 21 Miglietta, M. M., and R. Rotunno, 2010: Numerical Simulations of Low-CAPE Flows  
22 over a Mountain Ridge. *J. Atmos. Sci.*, **67**, 2391–2401 doi:  
23 <http://dx.doi.org/10.1175/2010JAS3378.1>.
- 24 Molini, L., A. Parodi, N. Rebor, and G. C. Craig, 2011: Classifying severe rainfall  
25 events over Italy by hydrometeorological and dynamical criteria, *Quart. J. Roy. Meteor.*  
26 *Soc.*, **137**, 148–154.
- 27 Moncrieff, M. W., and Changhai L., 1999: Convection Initiation by Density Currents:  
28 Role of Convergence, Shear, and Dynamical Organization. *Mon. Wea. Rev.*, **127**, 2455–  
29 2464. doi: [http://dx.doi.org/10.1175/1520-0493\(1999\)127<2455:CIBDCR>2.0.CO;2](http://dx.doi.org/10.1175/1520-0493(1999)127<2455:CIBDCR>2.0.CO;2).
- 30 Pastor, F., M. J. Estrela, D. Peñarrocha, M. M. Millán, 2001: Torrential Rains on the  
31 Spanish Mediterranean Coast: Modeling the Effects of the Sea Surface Temperature. *J.*  
32 *Appl. Meteor.*, **40**, 1180–1195.
- 33 Ricard, D.,V. Ducrocq, and V. Auger, 2012: A Climatology of the Mesoscale  
34 Environment Associated with Heavily Precipitating Events over a Northwestern  
35 Mediterranean Area. *J. Appl. Meteor. Climatol.*, **51**, 468–488.
- 36 Ryan, S., 2011:Storm Summary Number 01 for Potential Autumn Mid-Atlantic to  
37 Northeast U.S. Major Winter Storm", *NCEP Hydrometeorological Prediction Center*.
- 38 Romero, R., C. A. Doswell III, and C. Ramis, 2000: Mesoscale Numerical Study of Two  
39 Cases of Long-Lived Quasi-Stationary Convective Systems over Eastern Spain. *Mon.*  
40 *Wea. Rev.*, **128**, 3731-3751.



1 Roth, G., Barrett, E., Giuli, D., Goddard, J., Llasat, M.C., Minciardi, R., Mugnai, A.,  
2 Scarchilli, G. and Siccardi, F., 1996: The STORM Project: aims, objectives and  
3 organisation. *Remote Sensing Reviews*, **14**, 23-50.

4 Rotunno, R., and R. Ferretti, 2001: Mechanisms of intense Alpine rainfall. *J. Atmos. Sci.*,  
5 **58**, 1732–1749.

6 Siccardi, F., 1996: Rainstorm hazards and related disasters in the western Mediterranean  
7 region. *Remote Sens. Rev.*, **14**, 5–21.

8 Simmons A, Uppala C, Dee D, Kobayashi S., 2007: ERA-Interim: New ECMWF  
9 reanalysis products from 1989 onwards, *ECMWF Newsl.*, **110**, 25–35.

10 Trenberth, K., 2005: Uncertainty in hurricanes and global warming, *Science*, **308**, 1753–  
11 1754.

12 Tripoli, G. J., C. M. Medaglia, S. Dietrich, A. Mugnai, G. Panegrossi, S. Pinori, E. A.  
13 Smith, 2005: The 9–10 November 2001 Algerian Flood: A Numerical Study. *Bull. Amer.*  
14 *Meteor. Soc.*, **86**, 1229–1235.

15 Yu, C.-K., D. P. Jorgensen, and F. Roux, 2005: Multiple Precipitation Mechanisms over  
16 Mountains Observed by Airborne Doppler Radar during MAP IOP5. *Mon. Wea. Rev.*,  
17 **135**, 955–984.

18 Wang, J.-J., R. M. Rauber, H. T. Ochs III, and R. E. Carbone, 2000: The Effects of the  
19 Island of Hawaii on Offshore Rainband Evolution. *Mon. Wea. Rev.*, **128**, 1052-1069.

20

21

22

# 1 List of Figures

2

3 Figure 1. Topography and vertical sections of the affected areas.

4

5 Figure 2. Synoptic situation on October 25<sup>th</sup> 2011. From top to bottom: a) GFS reanalyses  
6 map for the 00UTC geopotential field at 500 hPa , b) airmass RGB (EUMETRAIN) at  
7 00UTC and c) water vapor 6.2 channel (EUMETRAIN) at 00UTC (courtesy of  
8 EUMETRAIN, which is an international training project sponsored by EUMETSAT, to  
9 support and increase the use of meteorological satellite data).

10

11 Figure 5. Radar reflectivity patterns of the October 25<sup>th</sup> 2011 (10:00 UTC) precipitation  
12 structure . a) 2000m CAPPI ; b) S-N transect ; c) E-W transect; d) SW-NE transect.

13

14 Figure 6. Persistence of the October 25<sup>th</sup> 2011 structure referenced to 8:00 UTC to  
15 indicate the period of time (between 8:00 UTC and 15:00 UTC) where reflectivity was  
16 above a 40 dB threshold. .

17

18 Figure 7. October 25<sup>th</sup> 2011. From left to right: a) enhanced IR10.8 channel from  
19 EUMETRAIN at 12UTC, b) severe storm RGB channel (EUMETRAIN) at 12UTC, c)  
20 cloud top temperature and height (CTTH) product (EUMETRAIN) at 12UTC (Courtesy  
21 of EUMETRAIN).

22

23 Figure 8. October 25<sup>th</sup> 2011. Geo-location of the three analyzed rain gauges:  
24 Brugnato/BorghettoVara, Santa Margherita Vara and Serò di Zignago. In the lower right  
25 corner, the port of La Spezia on eastern Liguria.

26

27 Figure 9. October 25<sup>th</sup> 2011. Comparison of the three rain gauges located inside the area  
28 hit by the storm (see Figure 8). The hyetograph represents the hourly accumulations of  
29 the three rain gauges of Brugnato (orange), S.ta Margherita Vara (blue) and Serò di  
30 Zignago (purple) in the time windows between 8 and 16UTC. Courtesy of Liguria Civil  
31 Protection Agency.

32

33 Figure 10. October 25<sup>th</sup> 2011. Radar-derived rainfall depth from 9:00 UTC to 15:00 UTC  
34 (Italian Radar Network mosaic).

35

36 Figure 11. Synoptic situation on November 4<sup>th</sup> 2011. From top to bottom: a) GFS  
37 reanalyses map for the 00UTC geopotential field at 500 hPa , b) airmass RGB  
38 (EUMETRAIN) at 00UTC and c) water vapor 6.2 channel (EUMETRAIN) at 00UTC  
39 (courtesy of EUMETRAIN).

40

41 Figure 14. Persistence of the November 4<sup>th</sup>2011 structure referenced to 9:00 UTC to  
42 indicate the period of time (between 9:00 UTC and 15:00 UTC) where reflectivity was  
43 above a 40 dB threshold.

44

1 Figure 15. November 4<sup>th</sup>2011. From left to right: a) enhanced IR10.8 channel from  
2 EUMETRAIN at 12UTC, b), severe storm RGB channel (EUMETRAIN) at 12UTC, c)  
3 cloud top temperature and height (CTTH) product (EUMETRAIN) at 12UTC (courtesy  
4 of EUMETRAIN, which is an international training project sponsored by EUMETSAT,  
5 to support and increase the use of meteorological satellite data).

6  
7 Figure 16. November 4<sup>th</sup>2011. Position of two rain gauges located inside the area hit by  
8 the storm: OMIRL, on the Bisagno creek, and LIMET on the Rio Fereggiano whose main  
9 drainage channel is represented by a thick line (in grey the portion flowing in the culvert).  
10 The thin black line shows the Bisagno creek

11  
12 Figure 17. November 4<sup>th</sup> 2011. Comparison of two rain gauges located inside the area hit  
13 by the event (see Figure 16). The hyetograph represents the hourly accumulations.  
14 LIMET is a private weather station located in the district, courtesy of the Ligurian  
15 Association of Meteorology - LIMET. OMIRL is an official Weather Station located  
16 about 2 km far apart the first one, courtesy of the Liguria Civil Protection Agency (data  
17 courtesy of Liguria Civil Protection Agency and LIMET.)

18  
19 Figure 18. October 25<sup>th</sup> 2011: Sea Surface Temperature Anomaly by JPL-ROMS (left)  
20 and CNR-MED (right) displayed together with 24 hourly rainfall depth halo-regions  
21 (above 50 mm).

22  
23 Figure 19. November 4<sup>th</sup> 2011: Sea Surface Temperature Anomaly by JPL-ROMS(left)  
24 and CNR-MED (right) displayed together with 24 hourly rainfall depth halo-regions  
25 (above 50 mm).

26  
27 Figure 20. Temporal evolution of the convective adjustment time-scale ( $\tau_{CH}$ ) for the event  
28 of October 25<sup>th</sup> (upper panel, local time is UTC+1h) and November 4<sup>th</sup> (lower panel,  
29 local time is UTC+2h).

30  
31 Figure 21. Reanalyses from NOAA/NCEP Model corresponding to 12UTC of October  
32 25<sup>th</sup> (left column) and November 4<sup>th</sup> (right column). The marked low-mid troposphere  
33 positive vorticity is clear by comparing the geopotential height at 500hPa, 700hPa,  
34 850hPa and mean sea level (courtesy of NOAA/NCEP).

35

# 1 Tables

Station	Longitude [°E]	Latitude [°]
Cenesi	8.14	44.08
Castellari	8.27	44.15
Genova Centro	8.95	44.41
Cavi	9.38	44.31

2 Table 1. Geographical coordinates of a sample of the OMIRL coastal wind stations.  
3  
4

Stations/Raindepths	1h	3h	6h	12h	24
Brugnato/Borghetto	143	303	469	493	538
Serò di Zignego	58	133	227	269	303
S.ta Margherita Vara	40	107	168	243	274

5 Table 2. Rainfall depths accumulated on standard durations observed by the three stations  
6 in Vara Valley.  
7  
8

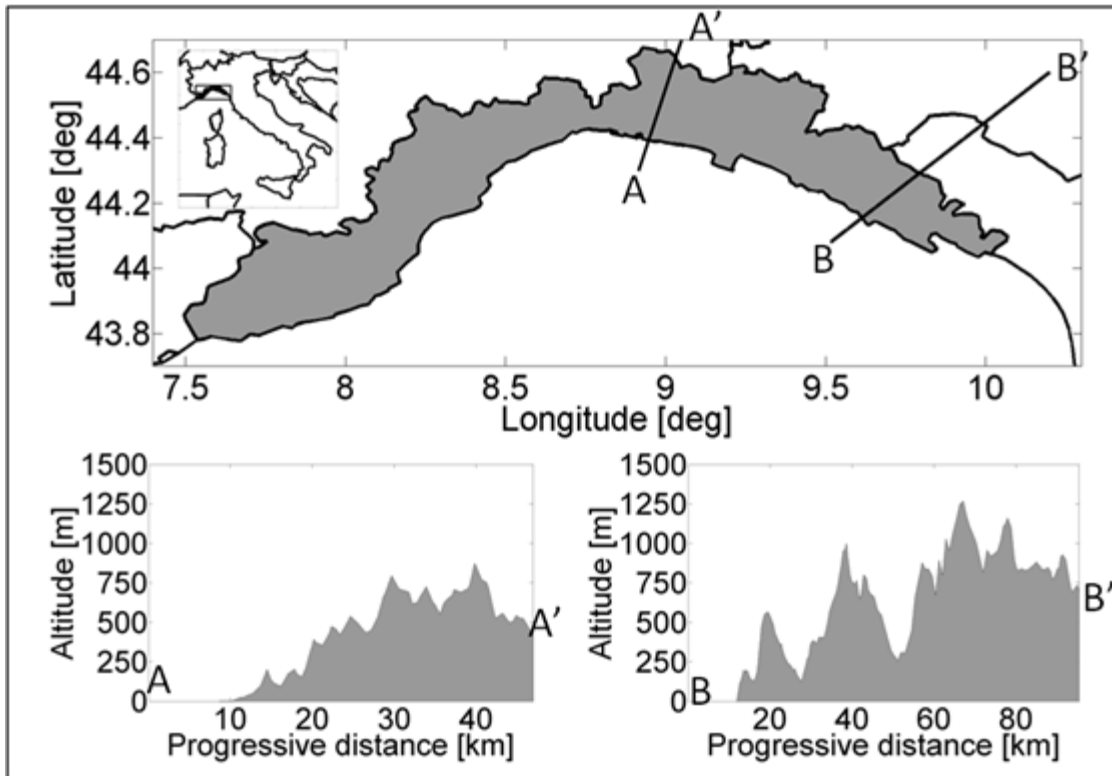
Stations/Raindepths	1h	3h	6h	12h	24
OMIRL	96	209	281	302	N.A.
LIMET	159	307	388	423	556

9 Table 3. Rainfall depths accumulated on standard durations observed by the two stations  
10 nearby the storm center.  
11  
12

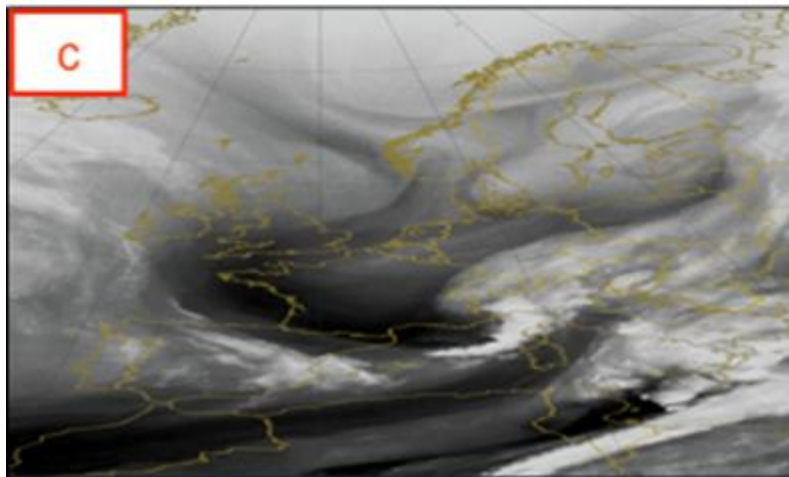
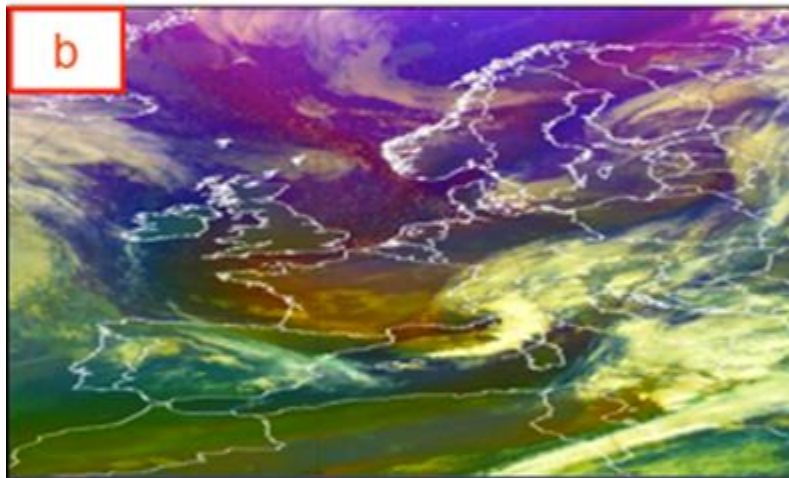
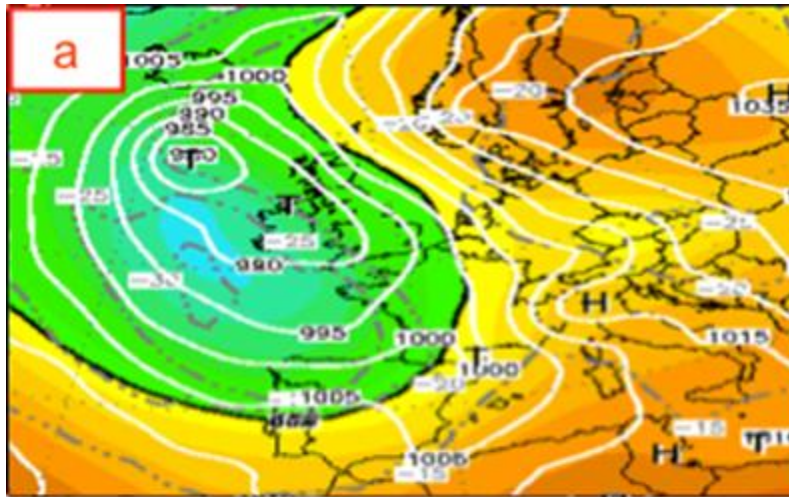
1 Figures

2

3



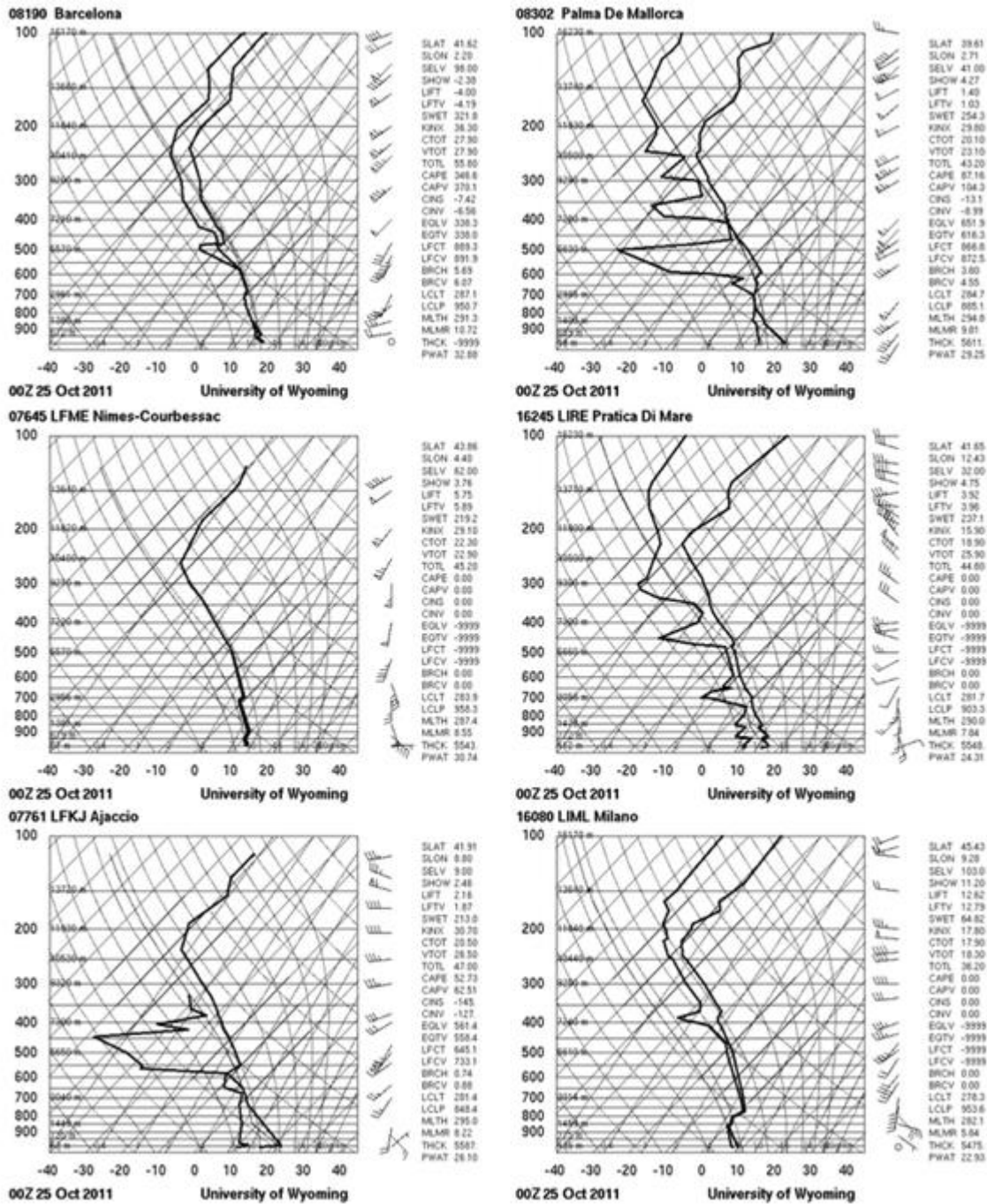
4 Figure 1. Topography and vertical sections of the affected areas.



1

2 Figure 2. Synoptic situation on October 25<sup>th</sup> 2011. From top to bottom: a) GFS reanalyses  
 3 map for the 00UTC geopotential field at 500 hPa , b) air mass RGB (EUMETRAIN) at  
 4 00UTC and c) water vapor 6.2 channel (EUMETRAIN) at 00UTC (courtesy of  
 5 EUMETRAIN, which is an international training project sponsored by EUMETSAT, to  
 6 support and increase the use of meteorological satellite data).

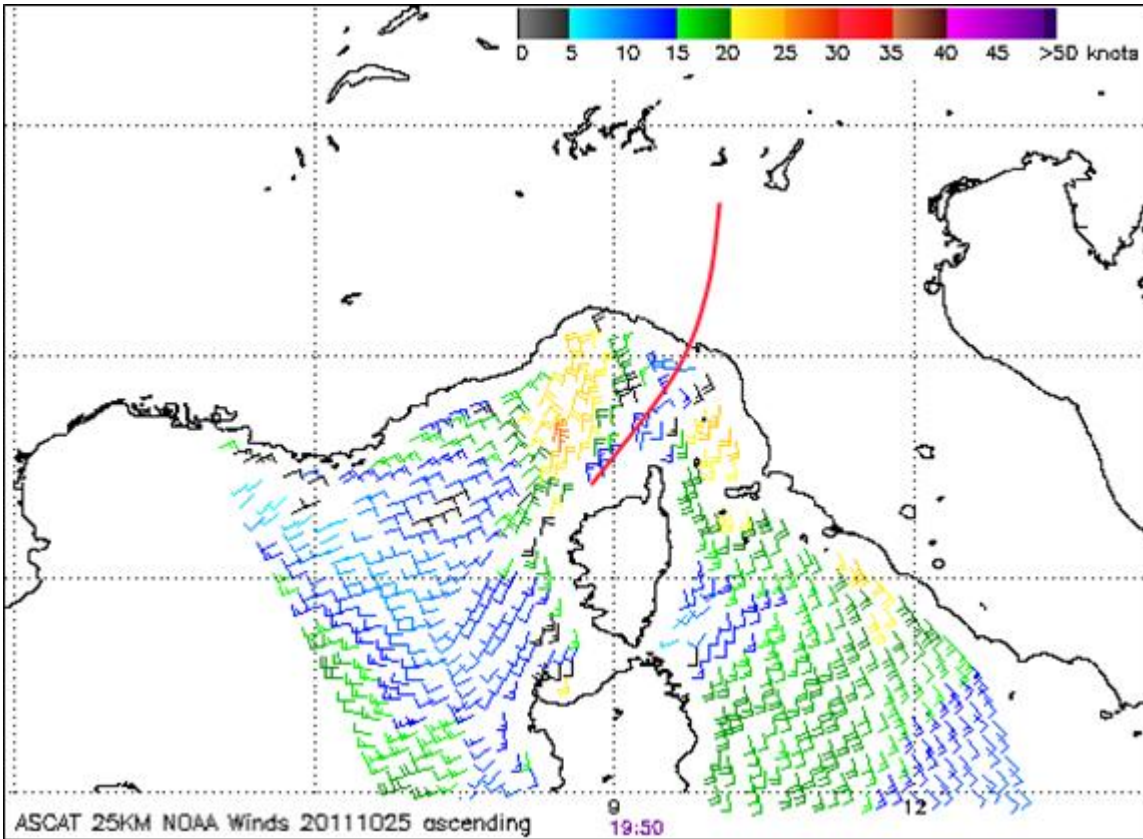
1  
2



3

4 Figure 3. Skew-T diagrams at 00UTC, 25 October 2011, for Barcelona, Palma de  
5 Maiorca, Nimes, Pratica di Mare, Ajaccio, and Milano Linate (courtesy of University  
6 of Wyoming - Department of Atmospheric Science).  
7

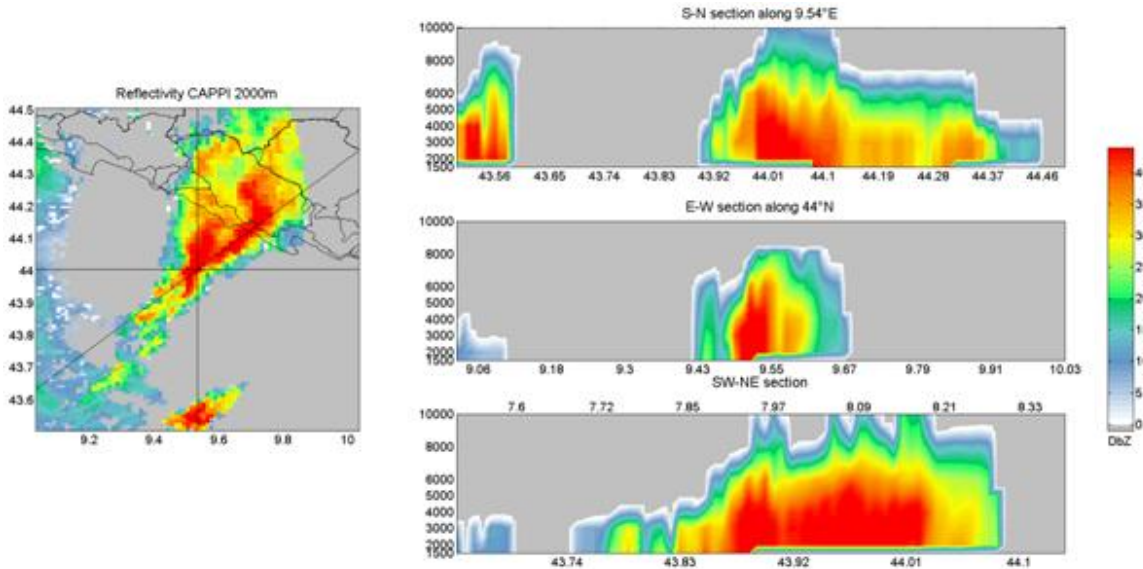




1

2 Figure 4:Advanced Scatterometer (ASCAT) ocean surface wind vectors data of 25km  
 3 resolution, on October 25 th 2011, ascending pass (20 UTC). The red line identifies the  
 4 low-level convergence zone of the windfield over the ocean.

5



6

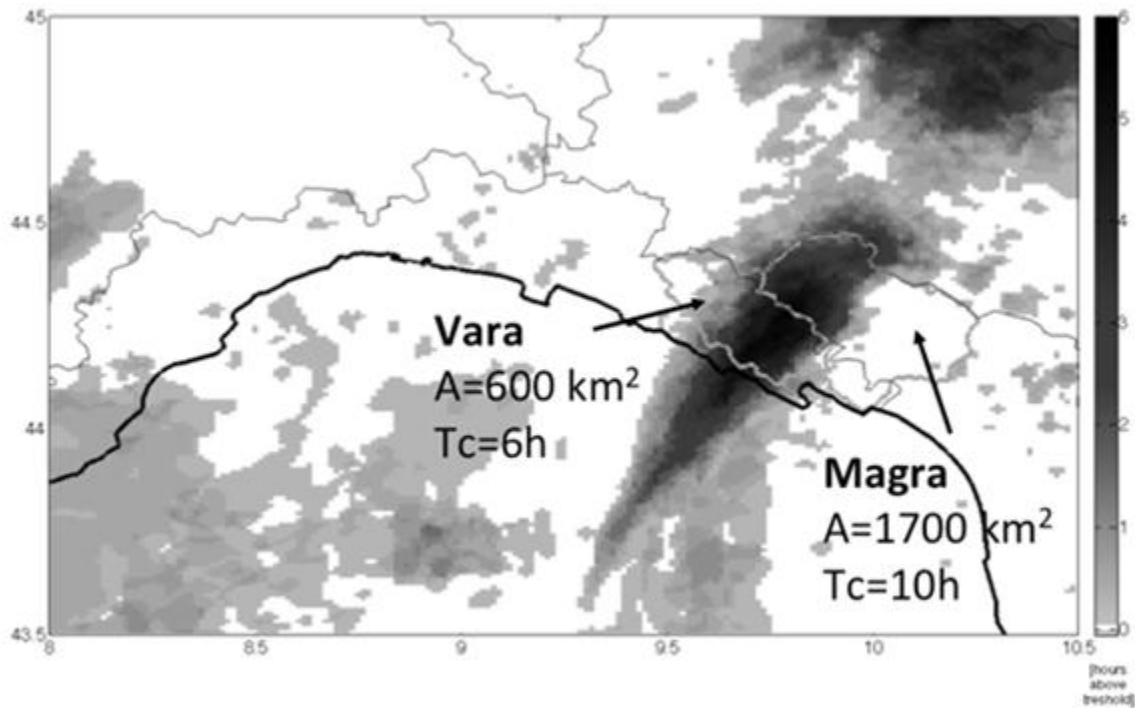
7 Figure 5. Radar reflectivity patterns of the October 25<sup>th</sup> 2011 (10:00 UTC) precipitation  
 8 structure . a) 2000m CAPPI ; b) S-N transect ; c) E-W transect; d) SW-NE transect.

9

10



1

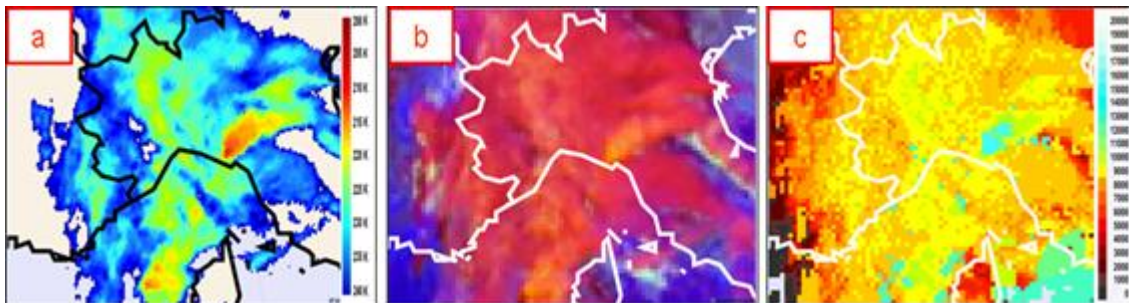


2 Figure 6. Persistence of the October 25<sup>th</sup> 2011 structure referenced to 8:00 UTC to  
3 indicate the period of time (between 8:00 UTC and 15:00 UTC) where reflectivity was  
4 above a 40 dB threshold. The Vara and Magra catchments mainly affected by the severe  
5 rainfall phenomena are depicted in the picture, together with the corresponding area and  
6 hydrological concentration time Tc.

7

8

9



10 Figure 7. October 25<sup>th</sup> 2011. From left to right: a) enhanced IR10.8 channel from  
11 EUMETRAIN at 12UTC, b) severe storm RGB channel (EUMETRAIN) at 12UTC, c)  
12 cloud top temperature and height (CTTH) product (EUMETRAIN) at 12UTC (Courtesy  
13 of EUMETRAIN).

14

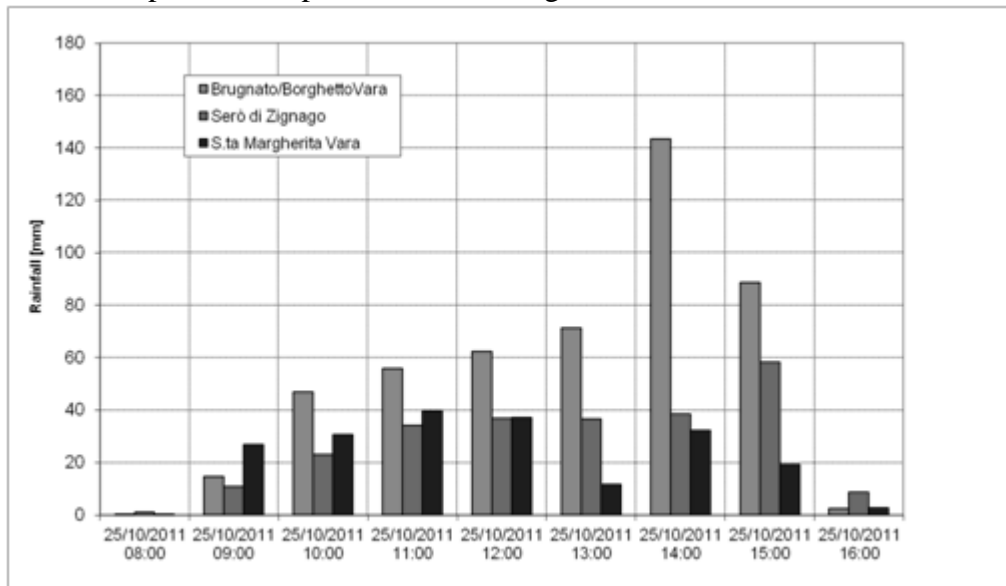
15

16



1

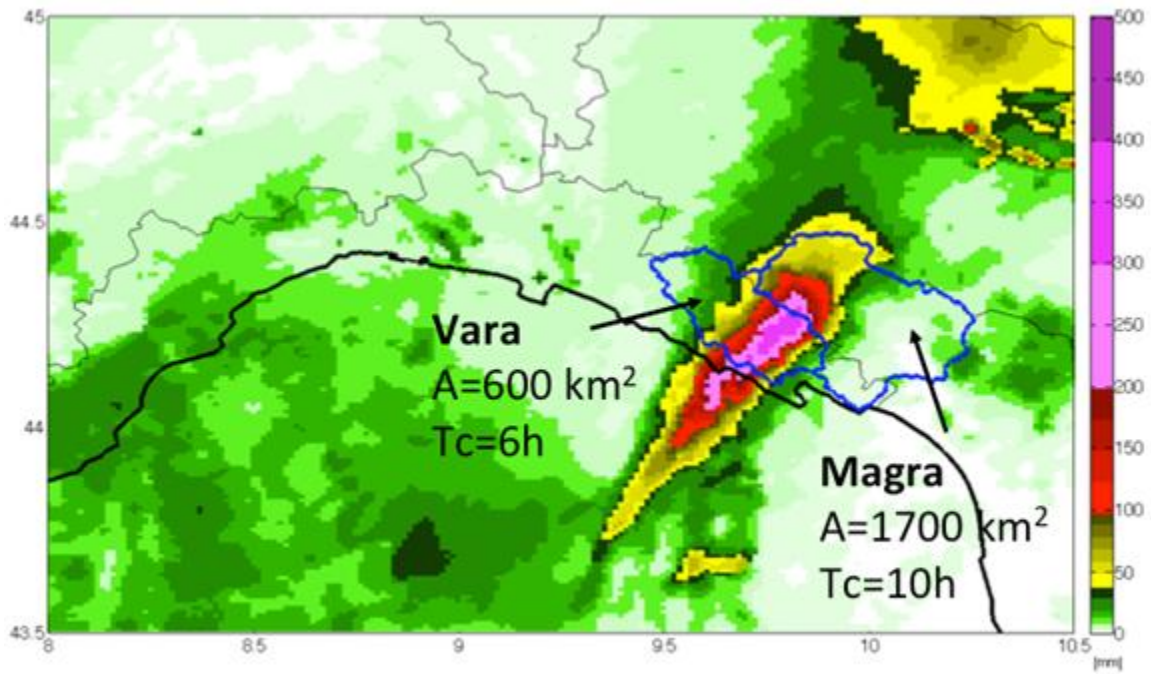
2 Figure 8. October 25<sup>th</sup> 2011. Geo-location of the three analyzed rain gauges:  
 3 Brugnato/BorghettoVara, Santa Margherita Vara and Serò di Zignago. In the lower right  
 4 corner, the port of La Spezia on eastern Liguria.



5

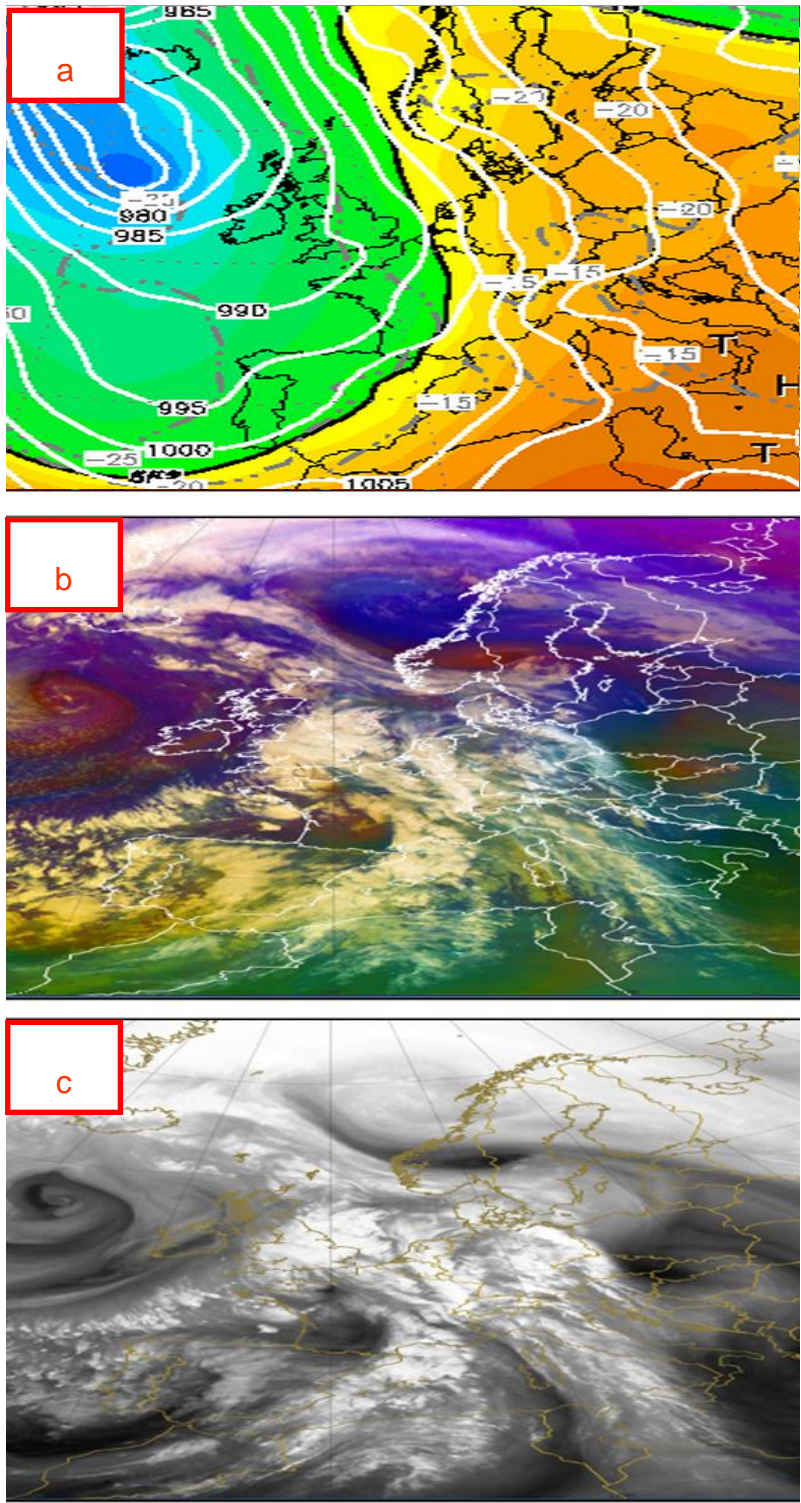
6 Figure 9. October 25<sup>th</sup> 2011. Comparison of the three rain gauges located inside the area  
 7 hit by the storm (see Figure 8). The hyetograph represents the hourly accumulations of  
 8 the three rain gauges of Brugnato (orange), S.ta Margherita Vara (blue) and Serò di  
 9 Zignago (purple) in the time windows between 8 and 16UTC. Courtesy of Liguria Civil  
 10 Protection Agency.

1



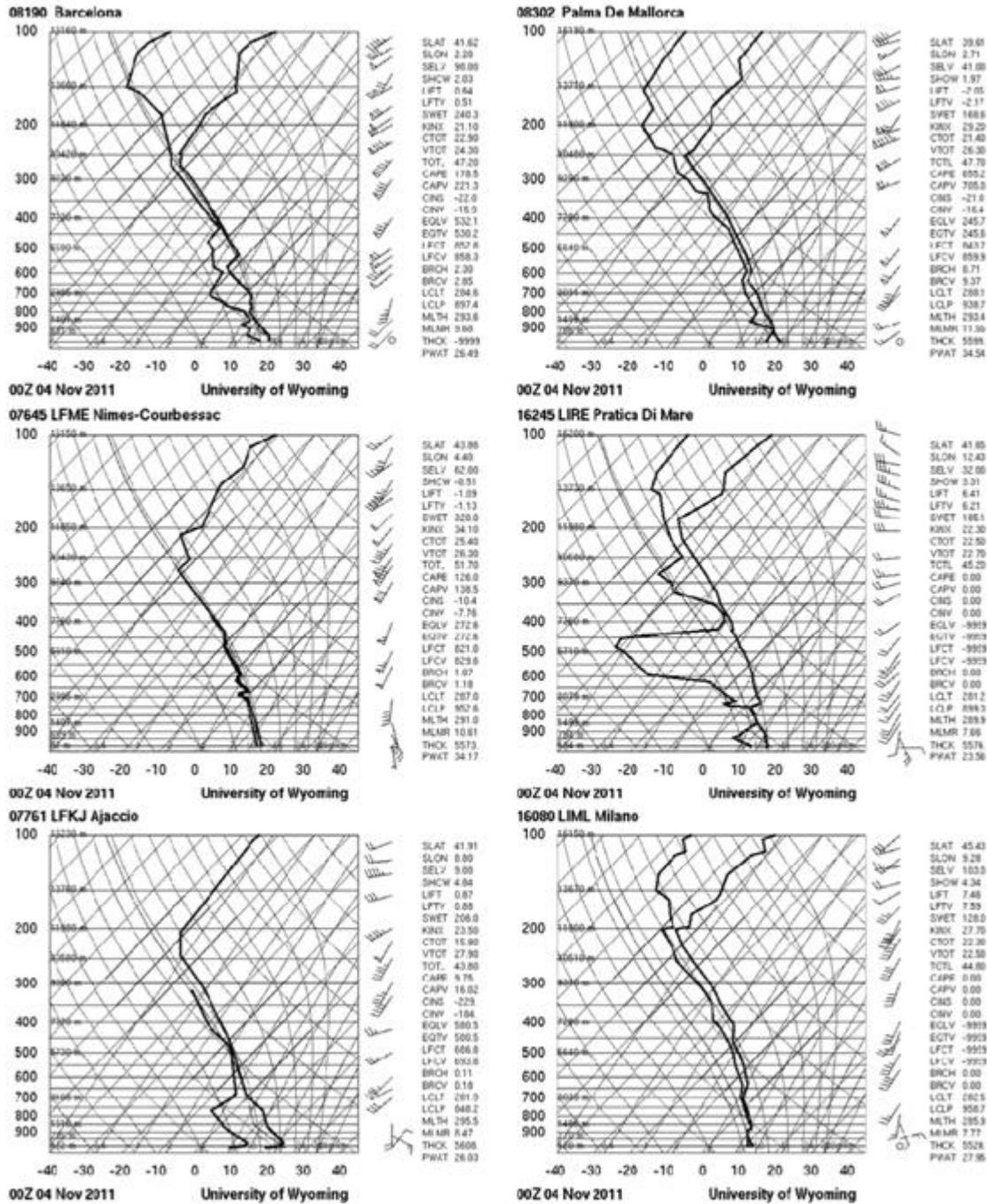
2 Figure 10. October 25<sup>th</sup> 2011. Radar-derived rainfall depth from 9:00 UTC to 15:00 UTC  
3 (Italian Radar Network mosaic). The Vara and Magra catchments mainly affected by the  
4 severe rainfall phenomena are depicted in the picture, together with the corresponding  
5 area and hydrological concentration time  $T_c$ .

6  
7  
8  
9



1  
 2 Figure 11. Synoptic situation on November 4<sup>th</sup> 2011. From top to bottom: a) GFS  
 3 reanalyses map for the 00UTC geopotential field at 500 hPa , b) airmass RGB  
 4 (EUMETRAIN) at 00UTC and c) water vapor 6.2 channel (EUMETRAIN) at 00UTC  
 5 (courtesy of EUMETRAIN).  
 6

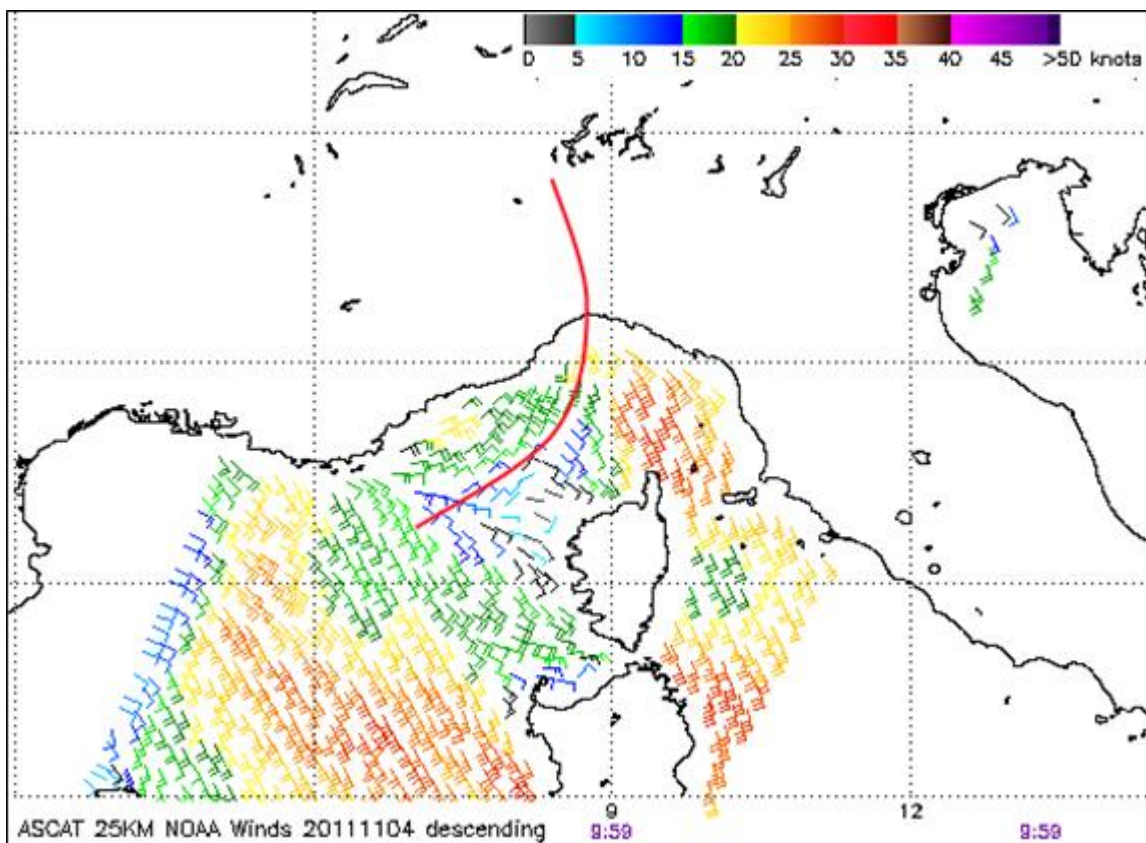




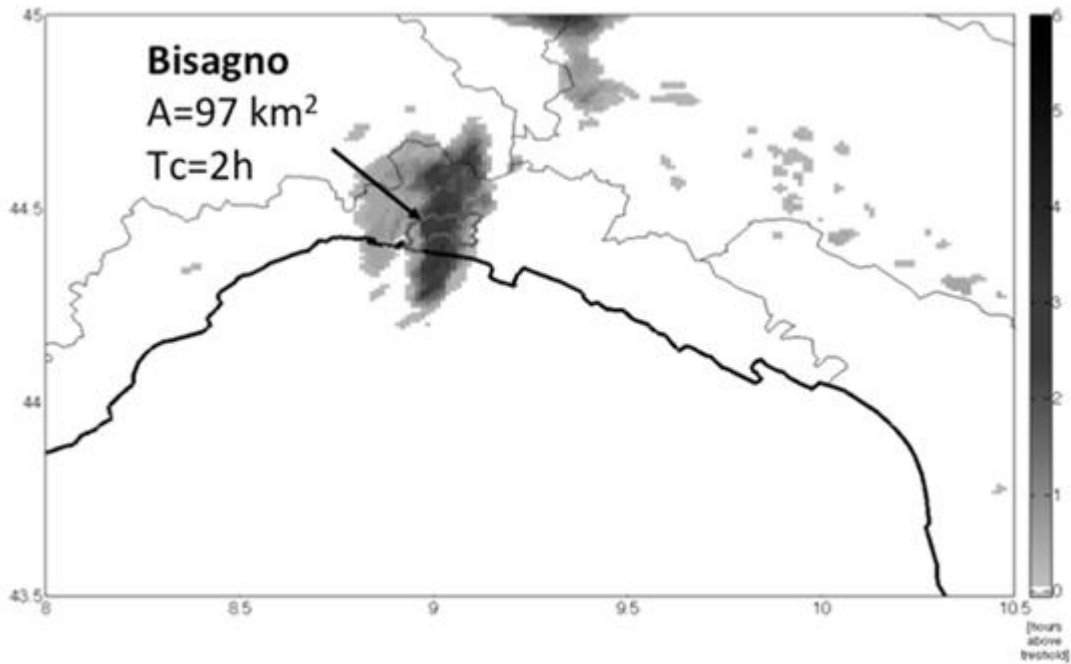
1

2 Figure 12. Skew-T diagrams at 00UTC, 4 November 2011, for Barcelona, Palma de  
 3 Maiorca, Nimes, Pratica di Mare, Ajaccio, and Milano Linate (courtesy of University  
 4 of Wyoming Department of Atmospheric Science).  
 5

1



2 Figure 13:Advanced Scatterometer (ASCAT) ocean surface wind vectors data of 25km  
3 resolution, on October 4th 2011, descending pass (10 UTC). The red line identifies the  
4 low-level convergence zone of the windfield over the ocean (courtesy of NOAA)

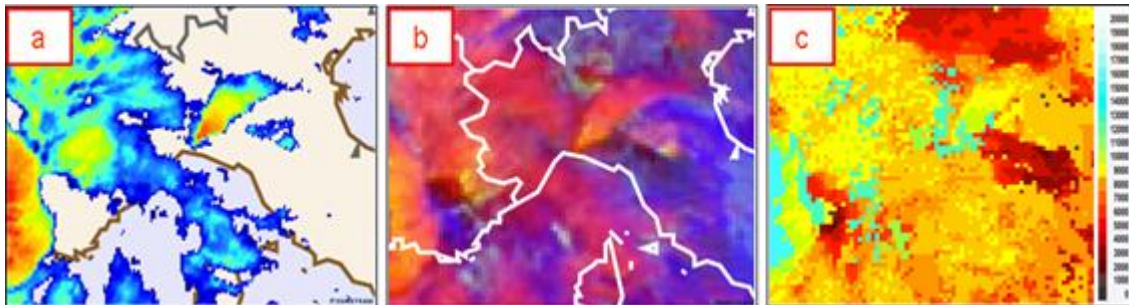


1

2 Figure 14. Persistence of the November 4<sup>th</sup>2011 structure referenced to 9:00 UTC to  
 3 indicate the period of time (between 9:00 UTC and 15:00 UTC) where reflectivity was  
 4 above a 40 dB threshold. The Bisagno catchment mainly affected by the severe rainfall  
 5 phenomena is depicted in the picture, together with the corresponding area and  
 6 hydrological concentration time Tc.

7

8



9

10 Figure 15. November 4<sup>th</sup>2011. From left to right: a) enhanced IR10.8 channel from  
 11 EUMETRAIN at 12UTC, b), severe storm RGB channel (EUMETRAIN) at 12UTC, c)  
 12 cloud top temperature and height (CTTH) product (EUMETRAIN) at 12UTC (courtesy  
 13 of EUMETRAIN, which is an international training project sponsored by EUMETSAT,  
 14 to support and increase the use of meteorological satellite data).

15

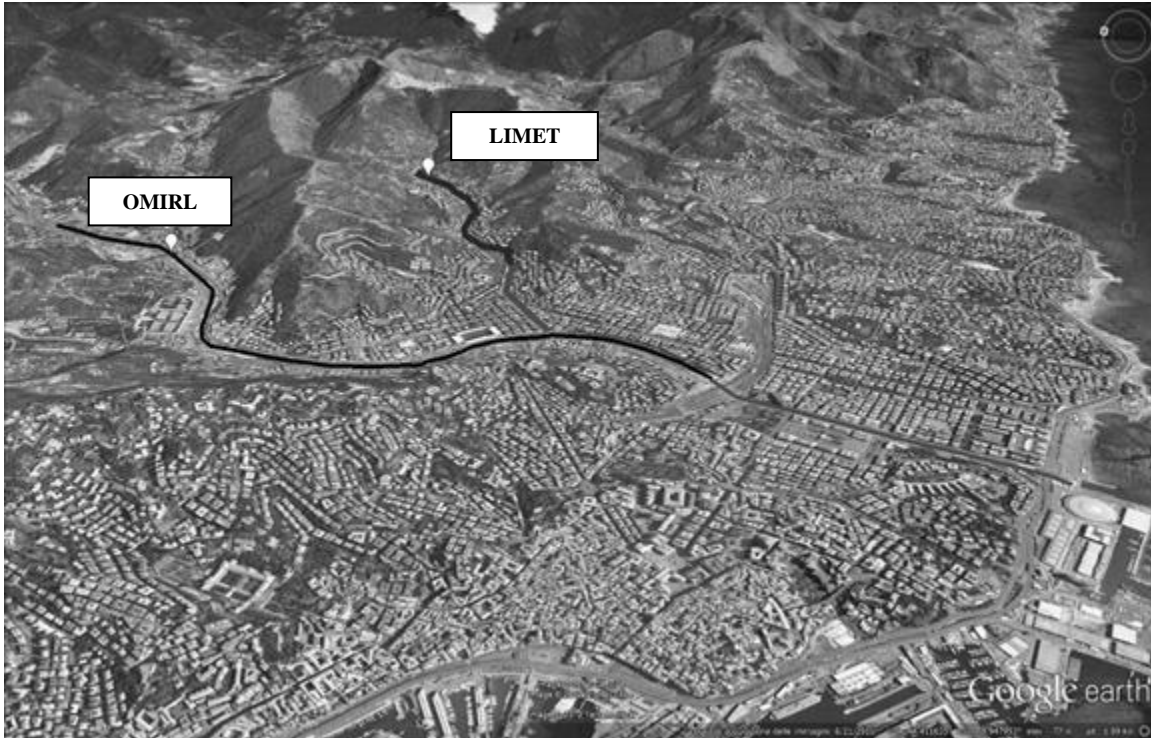
16

17

18

19

1  
2

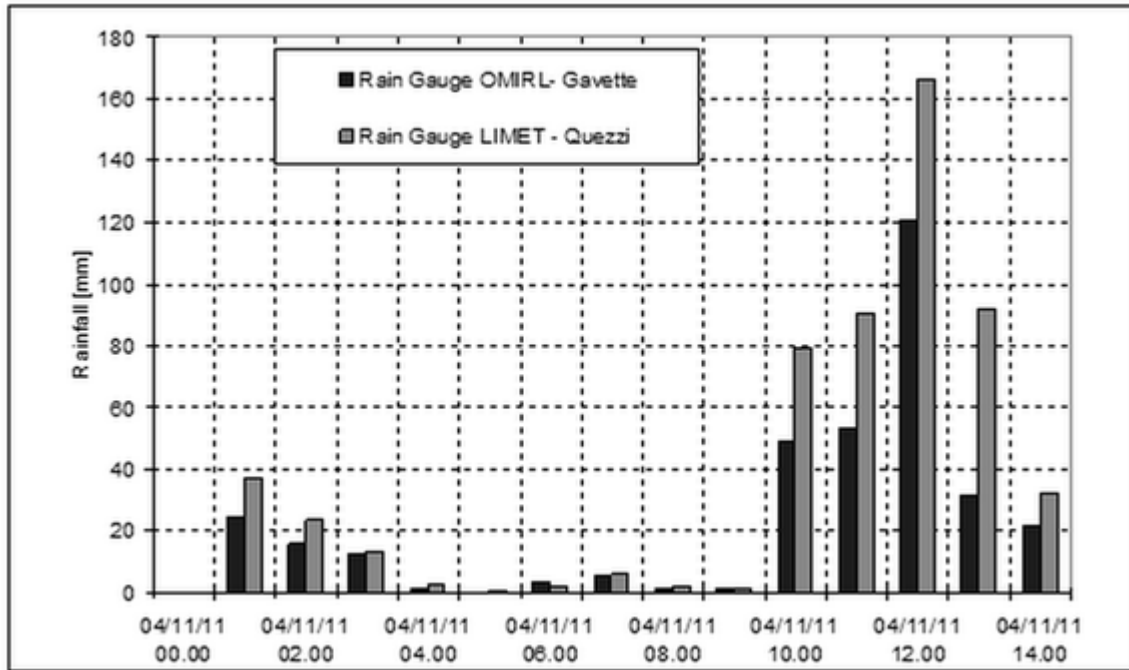


3

4 Figure 16. November 4<sup>th</sup> 2011. Position of two rain gauges located inside the area hit by  
5 the storm: OMIRL, on the Bisagno creek, and LIMET on the Rio Fereggiano whose main  
6 drainage channel is represented by a thick line (in grey the portion flowing in the culvert).  
7 The thin black line shows the Bisagno creek (in grey the portion flowing in the culvert).



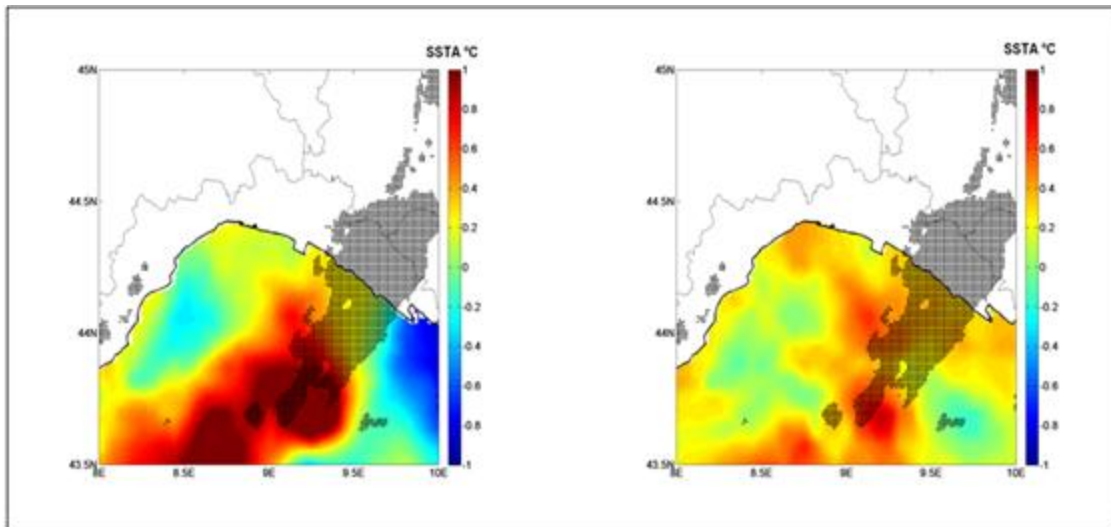
1



2

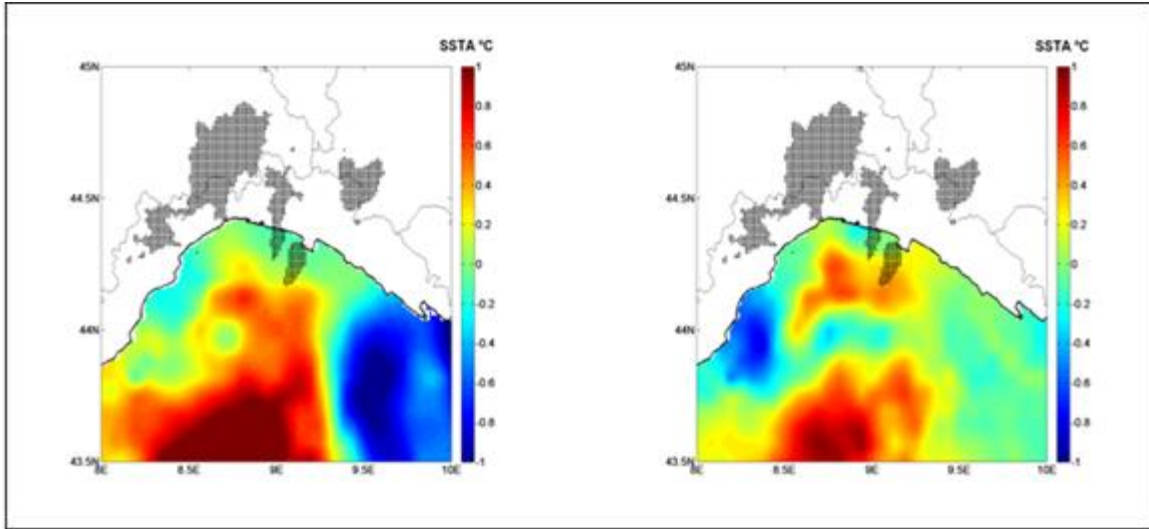
3 Figure 17. November 4<sup>th</sup> 2011. Comparison of two rain gauges located inside the area hit  
 4 by the event (see Figure 16). The hyetograph represents the hourly accumulations.  
 5 LIMET is a private weather station located in the district, courtesy of the Ligurian  
 6 Association of Meteorology - LIMET. OMIRL is an official Weather Station located  
 7 about 2 km far apart the first one, courtesy of the Liguria Civil Protection Agency (data  
 8 courtesy of Liguria Civil Protection Agency and LIMET.)  
 9

10



11 Figure 18. October 25<sup>th</sup> 2011: Sea Surface Temperature Anomaly by JPL-ROMS (left)  
 12 and CNR-MED (right) displayed together with 24 hourly rainfall depth halo-regions  
 13 (above 50 mm).  
 14

1



2 Figure 19. November 4<sup>th</sup> 2011: Sea Surface Temperature Anomaly by JPL-ROMS(left)  
3 and CNR-MED (right) displayed together with 24 hourly rainfall depth halo-regions  
4 (above 50 mm).

5

6

7

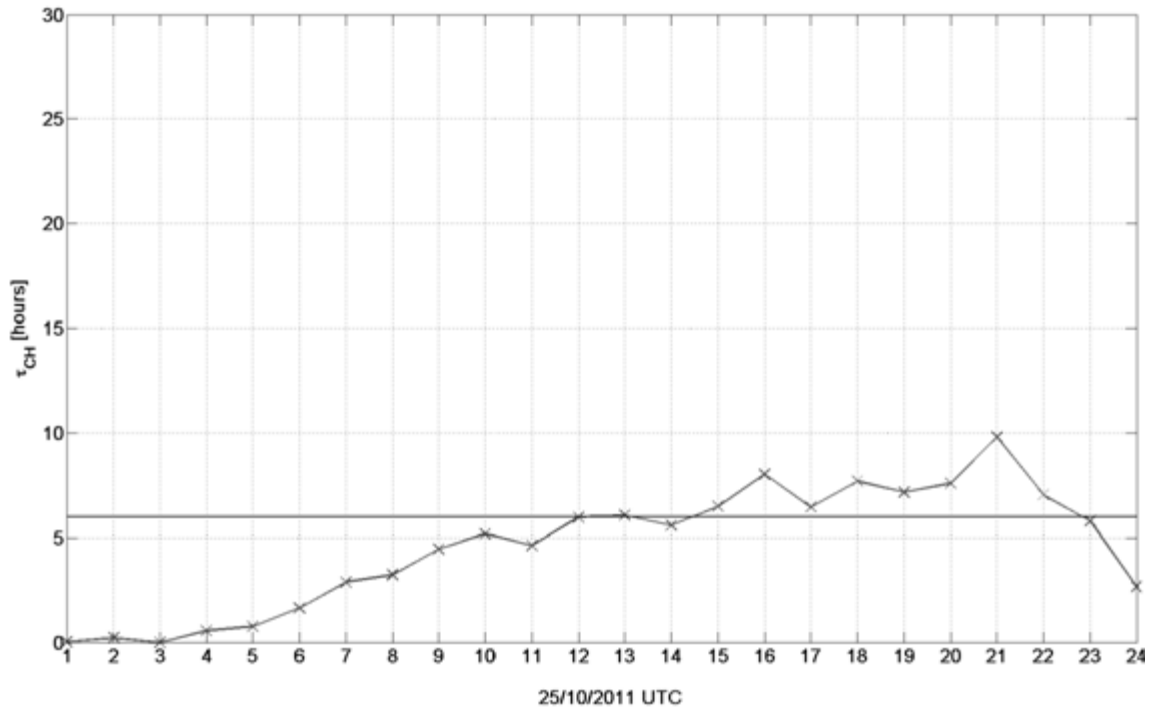
8

9

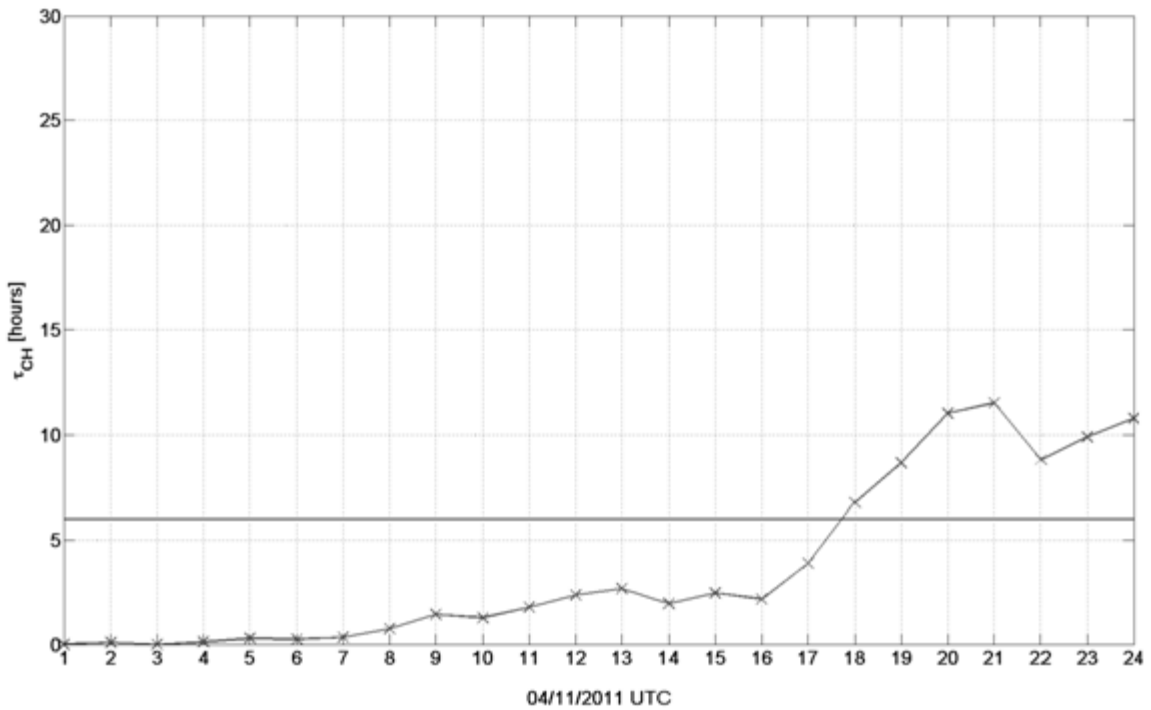
10

11

12



1



2 Figure 20. Temporal evolution of the convective adjustment time-scale ( $\tau_{CH}$ ) for the event  
 3 of October 25<sup>th</sup> (upper panel, local time is UTC+1h) and November 4<sup>th</sup> (lower panel,  
 4 local time is UTC+2h).

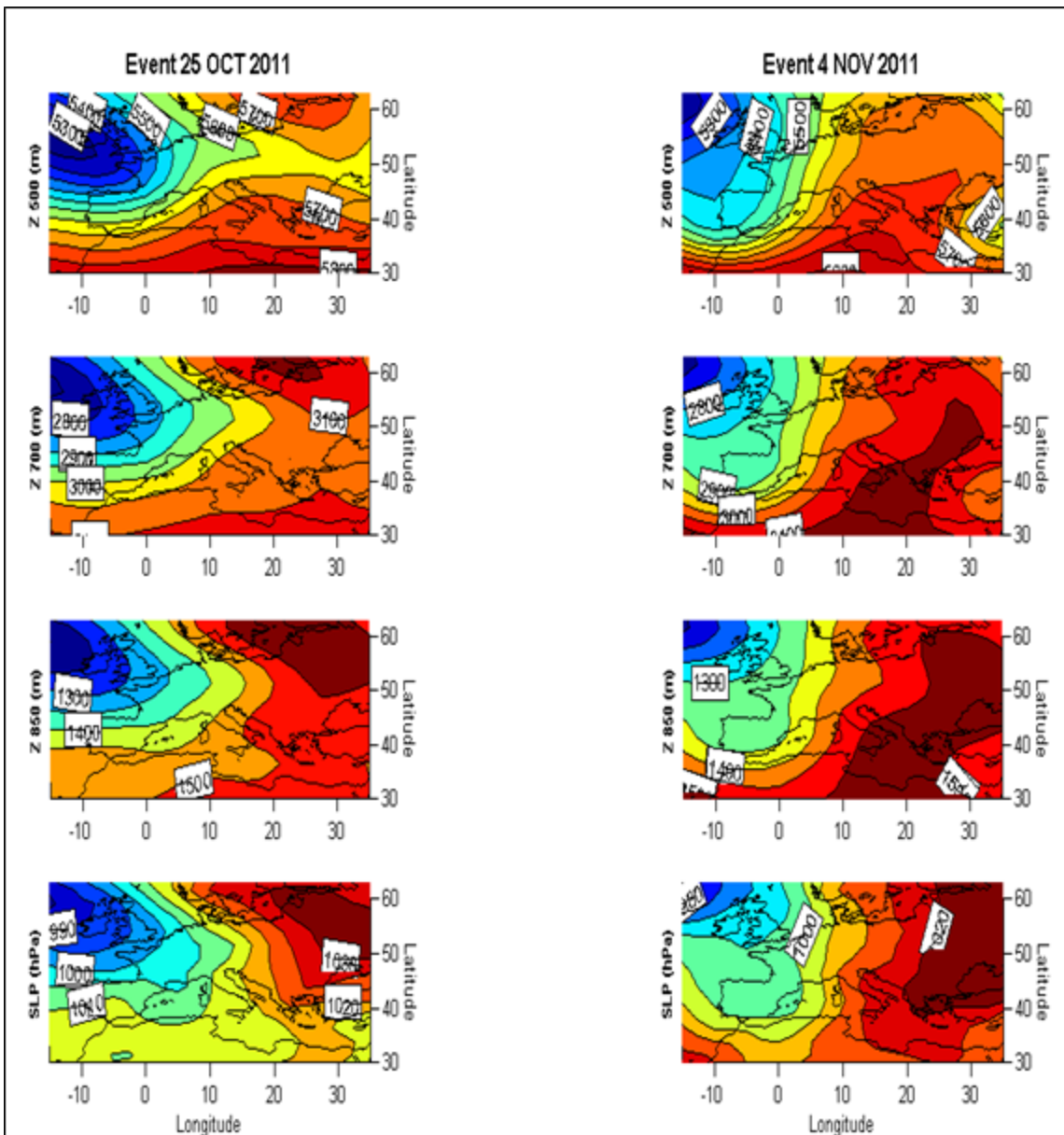


Figure 21. Reanalyses from NOAA/NCEP Model corresponding to 12UTC of October 25<sup>th</sup> (left column) and November 4<sup>th</sup> (right column). The marked low-mid troposphere positive vorticity is clear by comparing the geopotential height at 500hPa, 700hPa, 850hPa and mean sea level (courtesy of NOAA/NCEP).